# High- and low-temperature pyrolysis profiles describe volatile organic compound emissions from western US wildfire fuels

**Kanako Sekimoto[1,2,3,‡], Abigail R. Koss[1,2,4,*,‡], Jessica B. Gilman[1], Vanessa Selimovic[5], Matthew M. Coggon[1,2], Kyle J. Zarzana[1,2], Bin Yuan[1,2,6], Brian M. Lerner[1,2,†], Steven S. Brown[1,4], Carsten Warneke[1,2], Robert J. Yokelson[5], James M. Roberts[1], Joost de Gouw[1,2,4]**

[1] NOAA Earth System Research Laboratory (ESRL), Chemical Sciences Division, Boulder, CO 80305, USA

[2] Cooperative Institute for Research in Environmental Sciences, University of Colorado Boulder, Boulder, CO 80309, USA

[3] Graduate School of Nanobioscience, Yokohama City University, Yokohama, Kanagawa 236-0027, Japan

[4] Department of Chemistry and Biochemistry, University of Colorado Boulder, Boulder, CO 80302, USA

[5] Department of Chemistry, University of Montana, Missoula, MT 59812, USA

[6] Institute for Environment and Climate Research, Jinan University, Guangzhou, China

[*] Now at Department of Civil & Environmental Engineering, Massachusetts Institute of Technology, Cambridge, MA 02142, USA

[†] Now at Aerodyne Research, Inc., Billerica, MA 01821, USA

[‡]K. Sekimoto and A. Koss are equally contributing first authors.

*Correspondence to*: Kanako Sekimoto (sekimoto@yokohama-cu.ac.jp)

**Abstract.** Biomass burning is a large source of volatile organic compounds (VOCs) and many other trace species to the atmosphere, which can act as precursors to secondary pollutants such as ozone and fine particles. Measurements performed with a proton-transfer-reaction time-of-flight mass spectrometer during the FIREX 2016 laboratory intensive were analyzed with Positive Matrix Factorization (PMF), in order to understand the instantaneous variability in VOC

emissions from biomass burning, and to simplify the description of these types of emissions. Despite the complexity and variability of emissions, we found that a solution including just two emission profiles, which are mass spectral representations of the relative abundances of emitted VOCs, explained on average 85% of the VOC emissions across various fuels representative of the western US (including various coniferous and chaparral fuels). In addition, the profiles were remarkably similar across almost all of the fuel types tested. For example, the correlation coefficient $r^2$ of each profile between Ponderosa pine (coniferous tree) and Manzanita (chaparral) is higher than 0.84. The compositional differences between the two VOC profiles appear to be related to differences in pyrolysis processes of fuel biopolymers at high and low temperatures. These pyrolysis processes are thought to be the main source of VOC emissions. "High-temperature" and "low-temperature" pyrolysis processes do not correspond exactly to the commonly used "flaming" and "smoldering" categories as described by modified combustion efficiency (MCE). The average atmospheric properties (e.g. OH reactivity, volatility, etc) of the high- and low-temperature profiles are significantly different. We also found that the two VOC profiles can describe previously reported VOC data for laboratory and field burns.

## 1 Introduction

Biomass burning is a large source of volatile organic compounds (VOCs) and other trace species to the atmosphere. Reactions involving these VOCs produce ozone and fine particles, which are important air pollutants and radiative forcing agents (Alvarado et al., 2009; Alvarado et al., 2015; Yokelson et al., 2009; Jaffe et al., 2012). Some VOCs from fires also have direct health effects (Naeher et al., 2007; Roberts et al. 2011). Biomass burning occurs in wildfires, controlled burns of wildland and agricultural fuels, and in residential wood stoves and industrial processes. Given the variety of fuels and burning conditions, it is unsurprising that the VOC composition of biomass burning emissions varies greatly between different fire states, locations, and studies. Therefore, it is important to understand VOC emissions from biomass burning in detail and develop a predictive capability that explains some of the variability in VOC emissions.

Multiple complex processes take place in biomass burning, including (i) distillation with release of water vapor and terpenes, (ii) pyrolysis of solid biomass giving off flammable gases, (iii) flaming combustion, and (iv) non-flaming processes loosely lumped with smoldering

combustion such as glowing (gasification) of biomass (Yokelson et al., 1996; Yokelson et al., 1997; Collard and Blin, 2014; Liu et al., 2016). The main source of VOC emissions is pyrolysis of the polymers that form biomass such as cellulose, hemicellulose, and lignin. The temperature of the reaction and the physical characteristics of the biopolymer control which pyrolysis mechanism (e.g. depolymerization, fragmentation, or aromatization) is the main source of emitted VOCs (Yokelson et al., 1996; Yokelson et al., 1997; Collard and Blin, 2014; Liu et al., 2016). In a given fire, the processes (i)-(iv) occur simultaneously, but the relative importance of each process and temperature can change with time, which relates to the variability in integrated VOC emissions between different fires. This variability is often parameterized as a function of modified combustion efficiency (MCE = $\Delta CO_2/(\Delta CO+\Delta CO_2)$) (Yokelson et al., 1996). $CO_2$ and CO are representative gases emitted from the flaming and smoldering combustion processes, respectively, and are measured in most biomass burning studies. MCE is generally higher in flaming combustion (> 0.9) and lower in smoldering combustion (< 0.9) (Akagi et al., 2011).

The National Oceanic and Atmospheric Administration (NOAA) led the Fire Influence on Regional and Global Environments Experiment (FIREX) 2016 laboratory intensive conducted at the U.S. Forest Service Fire Sciences Laboratory in Missoula, Montana to study emissions of trace gases and aerosol from wildfires. Emissions from various fuels representative of the western U.S. were sampled under controlled conditions by extensive instrumentation (https://www.esrl.noaa.gov/csd/projects/firex/firelab/instruments.html). Experiments included so-called stack burns, in which emissions from an evolving burn were entrained into a large-diameter stack and sampled by various instruments. VOCs were measured by several instruments, including a PTR-ToF-MS (proton-transfer-reaction time-of-flight mass spectrometer) which captured gas-phase emissions with a fast time response during stack burns. The measurements show variability in VOC composition as the fire shifts between a dynamic mix of distillation, pyrolysis, flaming combustion, and "smoldering" combustion (here we use smoldering as a rough term to include various "non-flame" processes such as gasification). Ions measured with the PTR-ToF-MS were interpreted using a combination of gas-chromatographic pre-separation experiments, literature review, time-series analysis, and comparison to other instruments (Koss et al., 2018). Approximately 90% of the instrument signal could be attributed to identified VOCs.

The aims of this work are to understand the variation in gas-phase emissions both over the course of a fire and on a fire-integrated basis. Ultimately, this improved understanding of

emissions variability could be used to simplify predictions of the emission of secondary organic aerosol (SOA) and ozone precursors. To do this, the VOCs observed by PTR-ToF-MS in stack burns were analyzed using positive matrix factorization (PMF). We show that much of the observed variability in VOCs can be explained by only two factors, and that these two factors are qualitatively related to the temperature of the pyrolysis processes, which are the main sources of the VOC emissions from biomass burning. Based on this result, the two factors are named as a high-temperature pyrolysis factor and a low-temperature pyrolysis factor. The two factors are compared between fuels. Importantly, the high-temperature factor is quantitatively similar between different fuels, and the same is true for the low-temperature factor. The VOCs present in each factor are discussed in terms of composition, reactivity with OH, and propensity to form secondary organic aerosol. The relative importance of high- and low-temperature pyrolysis factors is quantified for each fuel and discussed with respect to physical properties of the fuel and the burn dynamics. We also investigate how well VOC emissions in biomass burning can be modeled by the two PMF emission profiles through comparisons with previously reported data from laboratory burns and wildfires. Finally, emissions of some specific compounds are discussed.

## 2 Methods

### 2.1 VOC measurements by PTR-ToF-MS

Fire emissions were measured during the FIREX 2016 intensive at the Fire Sciences Laboratory in Missoula, Montana. The facility consists of a large combustion chamber and has been described in detail previously (Christian et al., 2003; Christian et al., 2004; Burling et al., 2010).

VOC measurements were performed using several instruments, including a PTR-ToF-MS. This instrument employed a high-resolution ToF mass analyzer (Aerodyne Research Inc, MA, USA; Tofwerk AG, Thun, Switzerland) and measured with a time resolution of 2 Hz. VOCs and some inorganic compounds were ionized by proton transfer from $H_3O^+$ reagent ions. We include the inorganic compounds in the discussion of VOCs. Species with a proton affinity higher than that of water can be measured, which includes many unsaturated and polar compounds. The mass resolution of the instrument (3000-5000 FWHM m/Δm) was sufficient to determine the

elemental composition of ions and separate many isobaric compounds. Before each fire, background air in the combustion chamber was measured directly for several minutes. The instrument has been described in detail by Yuan et al. (2016; 2017), and operation, calibration, and peak identification during the FIREX 2016 laboratory intensive were described by Koss et al. (2018).

### 2.2 Fuel and biomass burn descriptions

Fifteen types of natural fuel mixtures, most of which are representative of important western U.S. ecosystems, were burned (Table 1). The names below are largely taken from the dominant plant species: (i) Ponderosa pine, (ii) Lodgepole pine, (iii) Loblolly pine, (iv) Douglas fir, (v) Engelmann spruce, (vi) Subalpine fir, (vii) Juniper, (viii) Bear grass, (ix) Ceanothus, (x) Chamise-contaminated, (xi) Chamise-uncontaminated, (xii) Manzanita-contaminated, (xiii) Manzanita-uncontaminated, (xiv) Sagebrush, and (xv) Excelsior (aspen wood shavings). "Contaminated" chaparral fuels (Manzanita and Chamise) were collected from a heavily air-polluted site near San Dimas, CA, while "uncontaminated" fuels were collected from a cleaner site in North Mountain, CA. Individual components of various fuel complexes, including canopy, litter, duff, and rotten wood, were also burned separately. Fuel moisture content ranged from 0.6% to 55.6%, and instantaneous MCE ranged from 0.75 to 1. Additional details on the fires and fuels are given by Selimovic et al. (2018) including: pre- and post-fire weight, weight of fuel components, and elemental composition (C, H, N, S, and Cl by weight). Each fuel type was burned several times. All fires consumed most of the fuel. The present experiments did not have a direct measurement of temperature within the fire, which is not homogeneous and therefore difficult to define. Rather, the air temperature of the emissions was measured by the FTIR instrument, located at the sampling inlet of the PTR-ToF-MS. The hot gases from the fire were mixed with air from the room, cooling the air significantly, but the trends in temperature are related to the initial temperature of the emitted gases.

### 2.3 PMF analysis

Data from 51 burns measured by PTR-ToF-MS (Table 1) were analyzed using positive matrix factorization (PMF), a numerical method that can be used to determine major compositional categories of emissions, their compositional profiles, and their relative

enhancements over time. PMF was conducted using the PMF Evaluation Tool v. 2.08A (Ulbrich et al., 2009). The basic principles of PMF and application to atmospheric chemistry measurements have been previously described (Ulbrich et al., 2009; Paatero and Tapper, 1994; Paatero, 1997).

More than 1000 ions were quantified in the PTR-ToF-MS mass spectra between *m/z* 12-217. Of these, 574 were selected for PMF analysis (Table S1). These 574 ions were resolved from neighboring peaks, were enhanced during at least one fire, and exclude primary (e.g., $H_3O^+$ and $H_3O^+(H_2O)$) and contaminant ions (e.g., Teflon fragments and transition metals) (Koss et al., 2018). The ion signals (in units of normalized counts-per-second; ncps), which are normalized to the $H_3O^+$ ion intensities and corrected for ToF-duty cycle, humidity dependence, and $H_3O^+$ ion depletion as described by Koss et al. (2018), were analyzed using PMF. Typically, raw ion signals in units of "counts-per-second (cps)" have been used for PMF analysis. However, cps VOC ion signals are affected by temporal variability (depletion and instability) in primary ion intensity and humidity during the fire. To obtain PMF results that exclude instrument effects, the normalized and corrected ion signals are used in this analysis. The uncertainties of the normalized and corrected ion signals were calculated based on those originating from the raw (cps) ion signals. We chose to use instrument signal rather than mixing ratio because many ion masses cannot be unambiguously related to a single VOC contributor: they have several contributors, or result from fragmentation, and cannot be converted to mixing ratio. For example, $C_7H_{13}^+$ (*m/z* 97.101) is a fragmentary product ion of at least five different VOCs, whose relative contributions are different between fires. However, variability in these ion signals still contains information useful for PMF. To interpret the PMF results, we did convert to mixing ratio where possible (Section 2.4). 528 compounds were quantified, of which 156 are identified VOCs. The PTR-ToF-MS measures 50-80% of total emitted non-methane VOC mass, with uncertainty in this value due to semivolatile compounds (Hatch et al., 2017).

In this work, we applied PMF to extended time series, in which all fires of a particular fuel type (e.g., Ponderosa pine) were consolidated into a single data matrix (Figure S1), as well as time series of single fire data. Each fuel type was burned several times. Some individual fires of a particular fuel did not necessarily capture the full possible range of high- and low-temperature fire conditions, because of variability in the relative amounts of fuel parts, fuel moisture content, when fuel was added, or other differences. PMF using the consolidated time series makes it

possible to capture the widest possible range of fire conditions. This approach also simplifies the comparison of average emission profiles between different types of fuels. Details on preparation of ion signal and uncertainty datasets are described in the Supporting Information (S1).

The discussion in Section 3 is based on the 2-factor PMF solutions. Out of the 574 ions, 434 ions were fitted well and together represented 99% of the total ion signal. A total of 140 ions were not well fitted as the difference between their measurements and the PMF reconstruction was higher than 50%; these ions are excluded from the factors presented here. Ulbrich et al. (2009) suggest that poor retrieval of ions with less than 5% of total signal is not uncommon.

### 2.4 Calculations of OH reactivity and volatility

To characterize key chemical properties of the emission profiles derived from PMF analysis, we compare the OH reactivity and volatility of VOCs in each profile. These calculations require conversion of the emission profiles from instrument signal (ncps) to mixing ratio (ppbv). Fragment ions, cluster ions, and ions not well fitted by PMF were excluded from the 574 ions used in PMF analysis and calibration factors were applied to the remaining 400 ions to convert them to mixing ratio. Of these, 156 have known VOC contributors, and account for 90% of the total instrument signal of non-primary and non-contaminant ions between *m/z* 12-217. (This corresponds to an average of 92% of the total VOC concentration detected by PTR-ToF-MS). Details on identification of the VOC contributors to ion masses and calibration are described by Koss et al. (2018).

We quantified the importance of the 156 identified ions to OH chemistry by multiplying the VOC + OH reaction rate coefficient ($cm^3$/molecule/sec) with the VOC fraction in the profile (ppbv VOC/ppbv of total VOC emitted) with a scaling factor to convert from VOC molar emission (ppbv VOC) to number density (molecule/$cm^3$ at experimental conditions of 900 mbar and 26°C). The resulting OH reactivity is in units of per second per ppbv of total VOCs measured with PTR-ToF-MS (1/sec/ppbv of total VOC emitted). For ions with more than one contributor, a weighted average rate constant was determined. Rate constants were taken from the literature (Atkinson and Arey, 2003; NIST Chemical Kinetics Database; Cicerone and Zellner, 1983; Gilman et al., 2015) or estimated from structurally similar VOCs. Details can be found elsewhere (Koss et al., 2018).

We also quantified volatility using the saturation concentration at 25 ºC ($C_0$, μg $m^{-3}$). Saturation concentrations were taken from the literature (Rumble, 2017-2018; NIST Chemistry WebBook; Yaws, 2015) where possible, and otherwise estimated based on the elemental composition of the ion (Li et al., 2016). Volatility determined from elemental composition is uncertain, especially for compounds with very low volatility where the uncertainty can be several orders of magnitude (Li et al., 2016). We determined volatility for the 400 non-fragmentary ions. We define volatility bins as follows, after Li et al. (2016): volatile organic compounds (VOC, $C_0 > 3\times10^6$ μg $m^{-3}$), intermediate volatility compounds (IVOC, $300 < C_0 < 3\times10^6$ μg $m^{-3}$), and semivolatile compounds (SVOC, $0.3 < C_0 < 300$ μg $m^{-3}$). Separation into such volatility bins is commonly used as an aid to discussion of SOA formation potential and gas/particle partitioning (Donahue et al., 2011).

## 3 Results and discussion

### 3.1 Two-factor parameterization of VOC emissions from biomass burning

Figure 1a shows the time series of selected VOC ion signals from burning a representative mixture of Ponderosa pine fuels. In these lab fires, total VOC emissions (red line in Figure 1a) often increase immediately and substantially during the initial combustion (for 170 seconds after starting the burn in this example), and then total emissions gradually decrease as the flames die out. Emissions of individual VOCs can be seen to fall into two categories: (i) higher emissions during the first part of the fire, e.g. naphthalene, which correlates with the PMF factor we will largely attribute below to high-temperature pyrolysis (blue line in Figure 1a), and (ii) higher emissions during the latter part of the fire, e.g., syringol, which correlates with the PMF factor we will attribute below to low-temperature pyrolysis (green line in Figure 1a). This separation into two categories is typical for most fires, with a few exceptions discussed later (e.g., burns of duff and rotten wood).

These two PMF factors (Figure 1b) describe the total VOC emissions remarkably well for most fuels: residuals (the differences between the measured ion signals and the calculated ion signals based on the PMF fits) are less than 15% on average, except for Douglas fir, Engelmann spruce, and Subalpine fir for which the residual average is 20-25%. The residuals for individual fuels are summarized in Table 1c. For most of the fuels, the time series of the first and second

247 factors are strongly correlated with those of naphthalene and syringol, respectively (correlation
248 coefficient ($r^2$) > 0.74). On the contrary, emissions of compounds mainly from flaming or non-
249 pyrolysis smoldering processes, such as CO, $CO_2$, and $NO_x$ (Figure 1c), do not correlate well
250 with the individual PMF factors (more detailed discussion is given in Section 3.5). This indicates
251 that the two PMF factors do not correspond to the flaming and smoldering combustion processes
252 that are described by MCE and often referenced in biomass burning literature. The main source
253 of VOC emissions is pyrolysis of fuel biopolymers, and *not* the flaming and/or other combustion
254 processes. Therefore, we primarily attribute these two factors to high-temperature pyrolysis and
255 low-temperature pyrolysis, respectively, and will use these names to describe these factors in this
256 work. Our association between the factors and pyrolysis temperature is related more rigorously
257 to the distribution of products observed as a function of pyrolysis temperature in the next section.
258 When allowing more than two factors in PMF, the time series and mass spectral profiles of the
259 additional factors can be represented as an "intermediate" or "splitting" of high- and/or low-
260 temperature factors which can be described by a linear combination of the two factors. As
261 examples, Figures S2 and S3 show the correlation between *n*-factor solutions ($n$ = 3, 4) and PMF
262 results from high- and low-temperature factors for Ponderosa pine datasets. This suggests that
263 only two factors, i.e., high- and low-temperature pyrolysis factors, were needed to explain most
264 of the variability we observed for the VOC emissions from biomass burning.
265 There are notable exceptions to the two-factor solution, including an infrequently observed,
266 but important, third factor that we call a "distillation" factor, and a fourth profile observed during
267 burns of duff. Several fires contain a distillation phase, in which a brief burst of VOCs, typically
268 enriched in terpenes, is emitted immediately prior to ignition. However, PMF captured this phase
269 for only a limited number of burns in which the distillation phase contained sufficient gas-phase
270 emissions and lasted long enough (~30 seconds). When a two-factor solution is used, the
271 terpenes are largely grouped with the high-temperature pyrolysis factor. Duff is defined as a
272 "layer of moderately to highly decomposed leaves, needles, fine twigs, and other organic
273 material found between the mineral soil surface and litter layer of forest soil" (Reardon, 2007).
274 The duff PMF solutions have residuals larger than 80% when solved with only two factors. This
275 means that duff burns have a unique VOC emission pattern that cannot be explained by only
276 high- and low-temperature factors. These exceptions are discussed in more detail later.
277

### 3.2 VOC emission profiles of high- and low-temperature pyrolysis factors

The mass spectral profiles of the relative abundances of emitted VOCs for the individual PMF factors obtained from a given fuel type are similar for replicate burns of the same fuel type. When comparing the PMF profiles for two individual burns of the Ponderosa pine realistic mixture, the correlation coefficient ($r^2$) is higher than 0.92 for both the high- and low-temperature pyrolysis factors (Figure 2a). Importantly, the mass spectra for the high-temperature pyrolysis factor are also very similar between different fuels, and the same is true for the low-temperature pyrolysis factor. For example, the correlations of each profile between (i) Douglas fir and Ponderosa pine, (ii) Manzanita (chaparral) and Ponderosa, and (iii) Bear grass and Ponderosa have a slope near 1 and $r^2 \geq 0.83$ (Figures 2b-d). In contrast, the correlation between the high- and low-temperature mass spectra is visually clearly lower ($r^2 < 0.69$,Figure 2e). Figure 3 shows the average VOC emission profiles of the two factors obtained using PMF results of 15 different fuels. The fractions of individual ion peaks in the emission profiles are summarized in Table S1. These average profiles are in good agreement with profiles of individual fuels: a best fit of $0.96 < \text{slope} < 1.04$ and $r^2 > 0.84$, except for high-temperature factor of Excelsior with $r^2 = 0.68$ (Table 1d and Figure S4). Excelsior is an unusual fuel in that it consists of fine shavings of a single fuel component (wood). VOC composition in high- and low-temperature profiles is discussed in Section 3.3.1.

The compositional differences between the two profiles can be qualitatively explained by the temperature of the pyrolysis reactions thought to be the main production mechanism of the VOCs, such as depolymerization, fragmentation, and aromatization (Yokelson et al., 1996; Yokelson et al., 1997; Collard and Blin, 2014; Liu et al., 2016). This is illustrated by the relative contributions from the high-temperature versus low-temperature factors for most emitted VOCs. VOCs expected from high-temperature processes have a higher emissions contribution from the high-temperature factor, and likewise for low-temperature VOCs and the low-temperature factor.

Figure 4a shows the contribution of each factor to selected pyrolysis products from major fuel biopolymers, i.e., hemicellulose, cellulose, and lignin. The contributions of individual VOCs are expressed by their normalized fractions ($F_{\text{high-T}}$ and $F_{\text{low-T}}$) of high- and low-temperature factors: $F_{\text{high-T}} = Fraction_{\text{high-T}}/(Fraction_{\text{high-T}} + Fraction_{\text{low-T}})$ and $F_{\text{low-T}} = Fraction_{\text{low-T}}/(Fraction_{\text{high-T}} + Fraction_{\text{low-T}})$, where $Fraction_{\text{high-T}}$ and $Fraction_{\text{low-T}}$ correspond to fractions (in ppbv/total VOC ppbv) of individual species in the high- and low-temperature VOC profiles

(Figure 3), respectively. Figure 4b also shows the relationship between pyrolysis temperature and representative products for individual biopolymers as reported in the literature (Collard and Blin, 2014). During the heating of biomass, different chemical bonds within the biopolymers are broken, which results in the release of VOCs and in rearrangement reactions within the matrix of the residue. Low temperature pyrolysis breaks the bonds between the monomer units of the polymers. Depolymerization in lignin (300-500 °C) produces guaiacols, (iso)eugenol, and syringol. Furans and furfurals are dominantly formed from cellulose and hemicellulose (300-400 °C). Emissions of these compounds have a larger contribution from the low-temperature factor ($F_{\text{low-T}}$ = 60-100%). Higher temperatures allow reaction of functional groups and covalent bonds in polymers and monomers. The resulting fragmentation emits various VOCs: for example, hydroxyacetone, acetaldehyde, and acetic acid from depolymerization of cellulose and/or hemicellulose. These VOCs have roughly equal contributions from low- and high-temperature factors. The release of oxygenated compounds during depolymerization and fragmentation increases the carbon percentage of the residual biopolymers. Benzene rings and aromatic polycyclic structures form, which is termed char. Higher temperature pyrolysis breaks progressively stronger bonds in char (> 500 °C). This aromatization process gives off aromatic compounds with short substituents (e.g., phenol), non-substituted aromatics (e.g., benzene), and polycyclic aromatic hydrocarbons (PAHs such as naphthalene). Most of those aromatics have a large contribution from the high-temperature factor ($F_{\text{high-T}}$ = 60-100%). As the temperature increases, substituents of the aromatic rings disappear and PAHs are dominantly produced. This is consistent with the contribution of the high-temperature factor to phenol ($F_{\text{high-T}}$ = 60%), benzene (77%), and naphthalene (92%).

These many diverse chemical processes are likely happening simultaneously during a fire, and their relative intensities may change based on fuel composition, fuel moisture content, or other as-yet poorly defined parameters. However, the net result of all these variables is the emission of just two major compositional groups. The VOCs that comprise these two groups mostly consist of the pyrolysis products described above and their analogs. During most of these fires, the emissions of any particular VOC can be described by a linear combination of the high-temperature and low-temperature pyrolysis time series. Some VOCs are emitted mainly from the high-temperature pyrolysis; some mainly from the low-temperature profile; and others have a mixed contribution. This is quantified by $F_{\text{high-T}}$ as described above. We sorted the VOCs by

$F_{high\text{-}T}$, to show how the chemical composition of emissions changes from high- to low-temperature pyrolysis process. Figure 5 shows the chemical characteristics of compounds that are mostly emitted in the high-temperature pyrolysis ($F_{high\text{-}T}$ = 80-100% in panel (a)), mostly emitted in the low-temperature pyrolysis ($F_{high\text{-}T}$ = 0-20% in panel (e)), or have mixed contributions from both pyrolysis ($F_{high\text{-}T}$ = 60-80% in panel (b), 40-60% in (c), and 20-40% in (d)). $F_{high\text{-}T}$ of each individual VOC is shown in Figure S5. In the category emitted mostly by the high-temperature pyrolysis, important compounds include alkyl-substituted aromatics and aliphatic alkenes (Figures 5a and b), whereas carbonyls have more equal contributions from the high- and low-temperature pyrolysis processes. It should be noted that terpenes (e.g., (oxygenated) monoterpenes and isoprene) emitted from distillation are grouped with the high-temperature pyrolysis (Figures 5a and b; Section 3.6).

Several nitrogen (N)-containing compounds also fall into high or low temperature categories consistent with behavior previously reported in the literature. The main N-containing compounds detected by PTR-ToF-MS are isocyanic acid (HNCO), nitrous acid (HONO), hydrogen cyanide (HCN), and ammonia ($NH_3$). HNCO, HONO, and HCN have a high contribution of the high-temperature factor ($F_{high\text{-}T}$ = 80-100% in Figure 5a), while $NH_3$ falls into the category with a large contribution from the low-temperature factor ($F_{low\text{-}T}$ = 86% in Figure 5e). Nitrogen in biomass typically exists as amino acids/proteins and pyrrole/pyridine (aromatic N-heterocycles). During the pyrolysis of those N-functionalities at high temperature (700-1100 °C), HCN is identified as the main product in most cases (Johnson and Kang, 1971; Haidar et al., 1981; Patterson et al., 1968; Houser et al., 1980). $NH_3$, resulting from the lower-temperature pyrolysis of proteins, has been classified as smoldering combustion gases and falls here into the low temperature profile (Yokelson et al., 1996).

The present analysis predominantly focuses on VOCs. The VOC emissions from biomass burning are dominated by pyrolysis reactions of biopolymers. However, not all species are emitted from pyrolysis reactions. For example, flaming combustion releases $CO_2$, $NO_x$, HONO, and black carbon, etc. This is a separate process and cannot be expected to be captured by our VOC framework. In Section 3.5 we show that MCE, which delineates flaming versus smoldering combustion, is a poorer descriptor of VOC variability than the high versus low-temperature pyrolysis framework.

### 3.3 Chemical characteristics of VOC emissions depending on pyrolysis temperature

#### 3.3.1 VOC composition

The VOC emission profiles for the high- and low-temperature factors are shown in Figure 3 and they mainly consist of hydrocarbons, oxygenates with $n$=1-7 oxygen atoms, and nitrogen- and/or sulfur-containing hydrocarbons (Figure 6). In each emission profile, about half of the fraction (in ppbv) is accounted for by a combination of the following seven compounds: (i) ethene ($C_2H_4$), (ii) formaldehyde (HCHO), (iii) methanol ($CH_3OH$), (iv) acetaldehyde ($CH_3CHO$), (v) acrolein ($CH_2$=CHCHO), (vi) acetic acid ($CH_3COOH$) and glycolaldehyde ($HOCH_2CHO$), and (vii) ammonia ($NH_3$). The other half includes several fundamental structures, with a variety of functionalities, as discussed later. Oxygenates with one oxygen are predominant in both emission profiles, accounting for 39% of molar emissions in the high-temperature profile and 36% in the low-temperature profile. Emissions of highly oxygenated compounds (≥ 2 oxygen atoms) and ammonia are higher in the low-temperature profile than in the high-temperature profile. The fractions of hydrocarbons and compounds that contain both N and O, such as HNCO, are lower in the low-temperature profile.

VOCs emitted from biomass burning can be generally organized into major structural groups: furans, aromatics, oxygenated aromatics, aliphatic compounds, and so on. Within each structural category, compounds can have various functionalities, such as alcohol or alkene substituents (Hatch et al., 2015). VOC composition classified by 11 structures and 17 functionalities is shown in Figures 7 and 8. Some VOCs have multiple functional groups. These are counted once in each relevant category. For example, guaiacol is counted in "Oxygenated aromatic" structural category as "Alcohol" and "Ether (methoxy)" functional groups.

The most dominant emissions are attributable to aliphatic oxygenates, i.e., 62% of molar emissions in the high-temperature profile and 60% in the low-temperature profile (Figure 7). This is due to the specific compounds (ii)-(vi) described above. The low-temperature profile is twice as rich in aromatic oxygenates (≥ 2 oxygen atoms) and furans as the high-temperature profile, while the high-temperature profile is enriched in aliphatic (mostly alkenes) and aromatic hydrocarbons. Terpenes (including isoprene, monoterpenes, sesquiterpenes, and oxygenated monoterpenes) emitted from distillation, not from pyrolysis, are dominantly grouped with the high-temperature factor. Compared to the low-temperature profile, the high-temperature profile is enriched in the following functional groups: C-C double bond (>C=C<), C-C triple bond (-

C≡C-), diene (>C=C-C=C<), polycyclic aromatic hydrocarbon (PAH), nitrile (-C≡N), amide (-C(=O)-N-), nitro ($-NO_2$), nitrate ($-NO_3$), thiol/sulfide (-S-(H)) (Figure 8). The low-temperature profile is enriched in alcohols (-OH), ethers (mostly methoxy groups: $-O-CH_3$), esters (-C(=O)-O-), and amines ($-NH_2$; mostly ammonia). The emissions of compounds with carbonyl groups (>C=O) and acids (-C(=O)-OH-) are similar. These results are consistent with the contributions of VOC to the high- and low-temperature factors described in Section 3.2.

### 3.3.2 OH reactivity

The hydroxyl radical (OH) is an important driver of daytime oxidation chemistry. Quantifying the VOC reactivity with OH provides insight into which VOC emissions may be most important for ozone and secondary organic aerosol (SOA) formation. Interestingly, the two profiles have a similar average per-molecule (weighted by abundance) rate constant with OH: $15.7\times10^{-12}$ $cm^3$/molecule/s for the high-temperature profile and $15.8\times10^{-12}$ $cm^3$/molecule/s for the low-temperature profile. However, the reactivity is provided by very different VOCs in each profile. Aliphatic oxygenates are important in both profiles, but more so in the high-temperature profile (30% of reactivity) than in the low-temperature profile (24% of reactivity). In the high-temperature profile, the reactivity also has a large contribution from terpenes and aliphatic hydrocarbons, while in the low-temperature profile, the reactivity is largely due to furans and aromatics (Figure 9a). Since the total VOC emissions in real-world fires come from a mixture of the high- and low- temperature pyrolysis factors, the total OH reactivity of fresh emissions should scale directly with VOC concentration.

### 3.3.3 Volatility

Volatility is another important chemical characteristic affecting secondary organic aerosol (SOA) yield and formation rate. The low-temperature emission profile contains more compounds that are of higher molecular weight, more oxygenated, and of lower volatility (Figure 9b). Oxygenated aromatics have been shown to be important biomass burning SOA precursors (Bruns et al., 2016), and while the SOA yields of many other compounds are unknown, the lower volatility and higher oxygen content of the low-temperature profile suggests a potentially more efficient SOA formation. SOA formation was also studied during the FIREX 2016 campaign, by oxidizing emissions in a chamber, and will be presented separately (Lim et al, in prep, 2018). We

note that the compounds with $C_0 < 10^2$ μg $m^{-3}$ shown in Figure 9b should be primarily in the particle phase and not measureable by PTR-MS without long delay times (Pagonis et al., 2017). However, the volatility of these compounds (calculated from the elemental composition) has an uncertainty of several orders of magnitude. Also, the cyclic compounds that are abundant in the low-temperature profile, such as aromatic oxygenates, produce multifunctional ring-opening-products that are known to be efficient SOA precursors (Yee et al., 2013). In a similar manner to the OH reactivity, the total volatility distribution can be estimated from the relative importance of the high- and low-temperature pyrolysis in a given fire.

### 3.4 Relationship of fuel characteristics to relative importance of high- and low-temperature pyrolysis factors

To use the PMF profiles (Figure 3) for estimates of VOC emissions from other fires, it is necessary to know the relative fire-integrated contributions of high- and low-temperature pyrolysis for those fires. As a step in this direction, in the present work, we found that fire-integrated molar emission ratios of total VOCs from high-temperature pyrolysis to low-temperature pyrolysis, $\sum VOC_{high\text{-}T}$ (in ppbv)/$\sum VOC_{low\text{-}T}$ (in ppbv), are related to which parts of the plants are burned (blue bars in Figure 10). When leafy fuels (i.e., canopy, shrub, and herbaceous fuels) are burned, the fraction of total VOC emissions originating from high-temperature pyrolysis is higher than those from low-temperature pyrolysis. These results imply that surface-to-volume ratios and the content of biopolymers in a given fuel can strongly affect the relative importance of high- and low-temperature pyrolysis. Leaves have high surface-to-volume ratios and despite higher fuel moisture, at least the surface may tend to heat up easily, resulting in a higher contribution from the high-temperature factor. The higher monoterpene content of foliage may explain why low-temperature distillation products like monoterpenes are associated with the high-T pyrolysis factor.

In contrast, the burn of rotten wood was found to contain VOC emissions from low-temperature pyrolysis only. Our brown rotten wood samples were enriched in lignin (Kirk and Cowling, 1984). Lignin is relatively resistant to thermal decomposition compared to cellulose and hemicellulose. The temperature range where pyrolytic decomposition occurs significantly is 280-500 °C for lignin, 240-350 °C for cellulose, and 200-260 °C for hemicellulose (Liu et al., 2016; Babu, 2008), as shown in Figure 4b. In our laboratory fires, the rotten wood first

smoldered for an extended period, and then flames were observed. However, only the low-temperature profile was observed. This suggests that it is more difficult for lignin-rich fuels to reach high enough temperatures to emit the "high-temperature pyrolysis" VOCs. Therefore, we do not see the same gradient in pyrolysis products that is observed for other fuel burns mainly consisting of cellulose and hemicellulose. Nitrogen content and speciation also vary between different biomass components, and temperature and differences in biopolymer content have been shown to strongly affect the composition of nitrogen-containing emissions (Hansson et al., 2004; Ren et al., 2011; Coggon et al. 2016). This is consistent with the observed differences in nitrogen speciation between the two profiles.

### 3.5 High- and low-temperature pyrolysis profiles describe total VOC emissions

Previous studies have found a correlation between the emission factors of certain VOCs and the fire-integrated modified combustion efficiency (MCE) (Yokelson et al., 1996: Yokelson et al., 1997; Selimovic et al., 2018). Thus, one might expect that the high- and low-temperature pyrolysis factors would also show a strong relationship to MCE. However, MCE does not parameterize the relative amounts of high- and low-temperature pyrolysis products very well, either instantaneously or on a fire-integrated basis (Figure 11). The basic reason is that $CO_2$ as well as $NO_x$ are emitted overwhelmingly from flaming combustion, which is *not* the main source of most VOC emissions, and these emissions are not expected to correlate with a linear combination of the high- and low-temperature pyrolysis processes, while CO emissions are reasonably well correlated with an average of high- and low-temperature emissions (Figures 1 and S6). This is especially clear in rotten log burns, where $CO_2$ and the PMF profiles are not correlated. The $CO_2$ emissions are enhanced by shifting from the smoldering to flaming combustion, but VOC emission patterns are not changed from the low- to high-temperature pyrolysis (Figure S7). Consequently, $CO_2$ and MCE, which indicate the separation between flaming and smoldering combustions, are not appropriate to estimate the high-/low-temperature pyrolysis VOC emissions. Our results indicate that VOC emissions are even more closely correlated to the biopolymer composition and the surface-to-volume ratios of fuels, than to the MCE. It is also seen that for some fires the air temperature correlates with the high-temperature contribution (e.g., Fires #37 and #59 shown in Figure S8a-c). This suggests that the VOC emissions are certainly related to the temperature within a fire. However, some other burns did

not have a good correlation between the temperature and VOC emissions (e.g., Fire #38 shown in Figure S8d), because the temperature measurement had some issues in the present work: (i) background temperature for each burn was different, (ii) some burns have colder temperature at end compared to start, which means that the laboratory was not controlled at constant temperature, and (iii) the increase in air temperature often lagged behind the emissions, especially at the start of a fire.

The relative contributions from the high- and low-temperature processes could be estimated from ratios of distinct marker species that are consistently enhanced in the high and low-temperature profiles. Several such pairs were considered and the ratio of ethyne ($C_2H_2$) to furan ($C_4H_4O$) can reasonably predict the ratio of high- to low-temperature emissions as given in Eq. 1:

$$\frac{total\ VOC\ ,high\ temperature\ (ppbv)}{total\ VOC\ ,low\ temperature\ (ppbv)} = \frac{ethyne\ (ppbv)\ /\ 0.0393}{furan\ (ppbv)\ /\ 0.0159} \quad (1)$$

The derivation and how the ethyne/furan ratio correlates with the high-/low-temperature emission ratio are given in the Supporting Information (S2 and Figure S9). However, this pair is not ideal because measurements of these two species are not frequently available and furan has high reactivity to both $O_3$ and $NO_3$ radicals. Future work should assess non-PTR measurements in order to find appropriate external markers.

Studies of laboratory burns and wildfires have reported variable emission ratios (or factors) for various VOCs as well as fire-integrated MCE, even for similar fuel types. Here we investigate how well total VOC emissions in biomass burning can be fit by the average VOC emission profiles (Figure 3) using emission factors and ratios reported in the literature for laboratory and field burns (Gilman et al., 2015; Stockwell et al., 2015; Akagi et al., 2011). When fitting the present high- and low-temperature factors to the other biomass burning data, total VOC emissions can be described with different relative fractions of the factors (Figure S10). For example, the best fit to a laboratory study by Gilman et al. (2015), using fuels from southwestern, southeastern, and northern U.S. (e.g., pine, spruce, fir, chaparral, mesquite, and oak) with MCE = 0.75-0.98, includes 32% high-temperature and 68% low-temperature VOC emissions; for another laboratory study by Stockwell et al. (2015) including several types of grass, spruce, and chaparral with MCE = 0.68-0.99, 59% high temperature and 41% low temperature; temperate forest fires (MCE = 0.95) reported by Akagi et al. (2011), 77% high temperature and 23% low

526 temperature, while in the case of chaparral fires (MCE = 0.96), 48% high temperature and 52%
527 low temperature. The fitting can be done with high correlation coefficient ($r \geq 0.92$) for all the
528 literature data (Figure S10). This is further evidence that at most two factors can explain the
529 majority of VOC variability. Therefore, these two factors could be used to fill in VOCs not
530 measured in the other studies which sometimes had less chemical detail. The current study
531 incorporated a wide range of MCEs and fuel moisture contents (Table 1), so the two-factor
532 description may be applicable under many conditions. However, some other factors should be
533 required for specific burns, as discussed below.
534
535 **3.6 Emission of specific compounds**
536 **3.6.1 Distillation phase**
537 At the beginning of many burn experiments, a white smoke is visible immediately prior to
538 ignition. This "distillation phase" does not result from pyrolysis or combustion, but rather a
539 gradual heating and release of water and volatile compounds trapped within the biomass. This
540 phase of the fire was not distinguished by PMF. The distillation phase from coniferous fuels is
541 enriched in some compounds highly relevant to atmospheric chemistry, especially terpenes (Koss
542 et al., 2018). But this phase lasts only a short time (typically less than 10 seconds), in which only
543 a short spike in emissions is observed. Accordingly, PMF cannot capture this phase effectively
544 even if a large number of factors is chosen. As an exception, the distillation phase of Sagebrush,
545 enriched in terpenes and a specific oxygenated monoterpene (camphor), can be distinguished as a
546 third PMF factor, because that phase lasted longer than 30 seconds in that fire. The reported
547 overall residual of 15% includes the poorly fitted distillation phase, and we stress that it typically
548 accounts for only a small portion of the overall emissions. Additionally, with the exception of
549 terpenes, the composition of the distillation profile is similar to that of the high-temperature
550 profile.
551 For some fuel burns other than coniferous fuels (e.g., Manzanita), VOC emissions during the
552 distillation phase are quite small, although distillation smoke is visible. In these cases, PMF
553 incorporates this phase into the low-temperature pyrolysis factor. There may be a relationship
554 between the VOC emission process coincident with distillation (low- or high-temperature) and
555 the presence of visible smoke. For instance, perhaps here the temperatures are low enough that
556 the compounds are able to re-condense into visible smoke.

### 3.6.2 Duff burn

A fourth factor can be resolved from the PMF analysis of duff burns. The distribution of VOC structures and functionality in the duff emission profiles (Figure 12a) is similar to the low-temperature pyrolysis profile (Figure 12b). The major difference is much higher emission of aliphatic nitrogen-containing compounds: 56% more of these compounds are emitted per-ppbv VOC in the duff profile than in the low-temperature profile. The additional emissions are mostly nitriles and amides, especially hydrogen cyanide (HCN), acetonitrile, and acetamide. Pyrroles and pyridines are also enhanced, but are much less abundant overall.

The organic portion of duff is enriched in nitrogen relative to other components of coniferous fuels. The nitrogen to carbon ratio in the Subalpine fir duff (N:C ratio = 0.028 by weight) was a factor of 2.1 higher than the average of other Subalpine fir components, and the Engelmann spruce duff N:C ratio (0.022) was 1.3 times higher than other Engelmann spruce components. Coggon et al. (2016), who investigated VOC emissions from the burning of herbaceous and arboraceous fuels, also found that the nitrogen-containing fraction of VOCs emitted from biomass burning increased with the nitrogen content of the fuel.

However, the nitrogen content cannot entirely explain why duff has a unique emission profile. Other fuels, such as Ceanothus and Ponderosa pine litter, have similar N:C ratios (0.025, 0.024, and 0.022, respectively) but are explained well by the 2-factor PMF solution consisting of high- and low-temperature pyrolysis factors. The contradiction may be due to differences in the speciation of nitrogen-containing organics. In woody and leafy fuels, proteins and amino acids account for 80-85% of the organic nitrogen (Ren and Zhao, 2015). In soils, proteins account for typically only 40% of organic nitrogen, and heterocyclic nitrogen compounds (pyrroles and pyridines) account for 35% (Schulten and Schnitzer, 1997). Pyrolysis of nitrogen heterocycles releases HCN, while proteins and amino acids may release more $NH_3$ (Leppälahti and Koljonen, 1995). This is consistent with the higher HCN and nitriles characteristic of the duff emission profile.

### 3.6.3 Variation in specific VOCs between fuels

When comparing emission profiles of individual fuels to the average profiles shown in Figure 3, there are some specific compounds whose emissions are notably higher (> ×5) or lower (< ×0.2) than the average (Figure S4). Here we highlight several key features:

(i) For Ponderosa/Lodgepole/Loblolly pines, Douglas/Subalpine firs, and Juniper, the emission of benzoquinone ($C_6H_4O_2 \cdot H^+$, *m/z* 109.028) is quite low in the high-temperature pyrolysis: 7-21% of the average emission for the pines and firs, and 2% for Juniper (Figures S4a-1~4, 6, and 7).

(ii) For fuels other than coniferous fuels and Sagebrush, i.e., Bear grass, Excelsior, Ceanothus, Chamise, and Manzanita, emissions of monoterpenes ($C_{10}H_{16} \cdot H^+$, *m/z* 137.132) are only 2-15% of the average (Figures S4a-8~14).

(iii) Excelsior emits especially low quantities of nitrogen-containing compounds, especially nitriles (hydrogen cyanide, acetonitrile, acrylonitrile, and propane nitrile) and pyridine, in the high-temperature pyrolysis (Figure S4a-9). This is because the nitrogen content in Excelsior is significantly lower than other fuels. The Excelsior N:C ratio (0.005 by weight) is 3.6 times lower than the average of other fuels (0.017 ± 0.006).

(iv) High-temperature pyrolysis of Ceanothus produces quite high emission of benzofuran-type compounds (Figure S4a-10). Benzofuran ($C_8H_6O \cdot H^+$, *m/z* 119.049) and methylbenzofuran and possibly its isomer such as cinnamaldehyde ($C_9H_8O \cdot H^+$, *m/z* 133.065) are 5.5 and 10.1 times higher than the average, respectively.

(v) Sagebrush specifically emits camphor ($C_{10}H_{16}O \cdot H^+$, *m/z* 153.127) in high-temperature pyrolysis (Figure S4a-15).

(vi) There are a limited number of exceptions in low-temperature profiles (Figure S4b). This means that low-temperature pyrolysis gives almost identical VOC emissions, independent of fuel types.

## 4 Conclusions

This work focused on interpretation of VOC emissions from biomass burning. We provided an understanding of VOC variability based on known chemical and physical processes to release VOCs from fires. We explained most of the observed variability between VOC emissions from fuel types and over the course of a fire using just two emission profiles: (i) high-temperature

pyrolysis profile and (ii) low-temperature pyrolysis profile. The results are summarized as follows:

1. The two profiles can explain the variability in VOC emissions composition between different fuel types and over the course of individual fires, with an average residual of < 15%.
2. The high-temperature profile is quantitatively similar between different fuel types ($r^2$ > 0.84), and likewise for the low-temperature profile.
3. The two profiles are significantly different in terms of VOC composition, volatility, and contributors to OH reactivity. The high-temperature pyrolysis profile is enriched in aliphatic unsaturated hydrocarbons, (polycyclic) aromatic hydrocarbons, terpenes (emitted from distillation), HCN, HNCO, and HONO. The resulting OH reactivity is primarily attributed to terpenes, aliphatic hydrocarbons, and non-aromatic oxygenates. The low-temperature pyrolysis profile is enriched in aromatic oxygenates, furans, and $NH_3$. The OH reactivity is contributed significantly by furans and aromatics.
4. The fire-integrated molar emission ratios of total VOCs from high-temperature pyrolysis to low-temperature pyrolysis are related to the biopolymer composition and surface-to-volume ratios of fuels. Higher surface-to-volume ratios lead to total VOC emissions enriched in products resulting from high-temperature pyrolysis than from those resulting from low-temperature pyrolysis.
5. The two VOC profiles can model previously reported VOC data for laboratory and field burns ($r \geq 0.92$). This suggests that these two profiles could be used to fill in VOCs not actually measured in the previous studies which sometimes had less chemical detail.
6. MCE, which parameterizes flaming and smoldering combustion, is not appropriate to estimate the high-/low-temperature pyrolysis VOC emissions. This suggests that the high- and low-temperature pyrolysis profiles may provide information on emissions that is not accessible with a broader definition of smoldering combustion implicit in the use of MCE.
7. Duff burns emit a specific VOC profile which is similar to that of low-temperature pyrolysis, but additionally includes aliphatic nitrogen-containing compounds, especially HCN, acetonitrile, and acetamide.

Our framework provides a way to understand VOC emissions variability in other laboratory and field studies of biomass burning. We highlight two areas of useful future work. First, external tracers should be found that will allow the prediction of the relative contribution of individual profiles. This could include specific chemical species, an understanding of how fuel or burn characteristics relate to the relative contribution of the two profiles, or a relationship between some measure of fire temperature and the VOC profiles. Second, the SOA and ozone formation potential of the two profiles should be determined. With this further work, the VOC profiles could be widely useful to model VOC emissions from many types of biomass burning in the western US, with additions to the framework being needed for fires that burn a lot of duff.

Future work should also include a quantitative comparison of the VOC PMF results to measurements of aerosol, inorganic gases, and organic species not measured by PTR-ToF-MS. Such a comparison would help define the relationship between VOCs and characteristics of primary organic aerosol (POA). We note that the primary aerosols have also been shown to have distinct profiles that correlate with different pyrolysis and combustion processes in the fire (Reece et al., 2017; Haslett et al., 2017).

**Acknowledgments**

K. Sekimoto acknowledges the Postdoctoral Fellowships for Research Abroad from Japan Society for the Promotion of Science (JSPS) and a Grant-in-Aid for Young Scientists (B) (15K16117) from the Ministry of Education, Culture, Sports, Science and Technology of Japan. A. Koss acknowledges support from the NSF Graduate Fellowship Program. M. Coggon acknowledges the Visiting Postdoctoral Fellowship from Cooperative Institute for Research in Environmental Sciences (CIRES). V. Selimovic and R. J. Yokelson were supported by NOAA-CPO grant NA16OAR4310100. J. de Gouw worked as a consultant for Aerodyne Research Inc. during part of the preparation phase of this manuscript. We thank for support from NOAA AC4 external funding, and thank the USFS Missoula Fire Sciences Laboratory for their assistance and cooperation. This work was also supported in part by NOAA's Climate Change and Health of the Atmosphere initiatives.

678 **References**

679 Akagi, S. K., Yokelson, R. J., Wiedinmyer, C., Alvarado, M. J., Reid, J. S., Karl, T., Crounse, J.
680 D., and Wennberg, P. O.: Emission factors for open and domestic biomass burning for use in
681 atmospheric models, Atmos. Chem. Phys., 11, 4039-4072, https://doi.org/10.5194/acp-11-
682 4039-2011, 2011.
683 Alvarado, M. J., Wang, C, and Prinn, R. G.: Formation of ozone and growth of aerosols in young
684 smoke plumes from biomass burning: 2. Three-dimensional Eulerian studies, J. Geophys. Res.,
685 114 (D9), D09307, http://doi.org/10.1029/2008JD011186, 2009.

686 Alvarado, M. J., Lonsdale, C. R., Yokelson, R. J., Akagi, S. K., Coe, H., Craven, J. S., Fischer, E.
687 V., McMeeking, G. R., Seinfeld, J. H., Soni, T., Taylor, J. W., Weise, D. R., and Wold, C. E.:
688 Investigating the links between ozone and organic aerosol chemistry in a biomass burning
689 plume from a prescribed fire in California chaparral, Atmos. Chem. Phys., 15 (12), 6667-6688,
690 http://doi.org/10.5194/acp-15-6667-2015, 2015.

691 Atkinson, R. and Arey, J. Atmospheric degradation of volatile organic compounds, Chem. Rev.,
692 103 (12), 4605-4638, http://doi.org/10.1021/cr0206420, 2003.
693 Babu, B. V.: Biomass pyrolysis: a state-of-the-art review. Biofuels, Bioprod. Bioref., 2, 393-414,
694 http://dpo.org/10.1002/bbb.92, 2008.
695 Bruns, E. A., El Haddad, I., Slowik, J. G., Kilic, D., Klein, F., Baltensperger, U. and Prévôt, A. S.
696 H.: Identification of significant precursor gases of secondary organic aerosols from residential
697 wood combustion., Sci. Rep., 6, 27881, doi:10.1038/srep27881, 2016.
698 Burling, I. R., Yokelson, R. J., Griffith, D. W. T., Johnson, T. J., Veres, P., Roberts, J. M.,
699 Warneke, C., Urbanski, S. P., Reardon, J., Weise, D. R., Hao, W. M., and de Gouw, J.:
700 Laboratory measurements of trace gas emissions from biomass burning of fuel types from the
701 southeastern and southwestern United States, Atmos. Chem. Phys., 10, 11115-11130,
702 https://doi.org/10.5194/acp-10-11115-2010, 2010.
703 Christian, T. J., Kleiss, B., Yokelson, R. J., Holzinger, R., Crutzen, P. J., Hao, W. M., Saharjo, B.
704 H., and Ward, D. E.: Comprehensive laboratory measurements of biomass-burning emissions:
705 1. Emissions from Indonesian, African and other fuels, J. Geophys. Res., 108 (D23), 4719,
706 http://doi.org/10.1029/2003JD003704, 2003.

Christian, T. J., Kleiss, B., Yokelson, R. J., Holzinger, R., Crutzen, P. J., Hao, W. M., Shirai, T., and Blake, D. R.: Comprehensive laboratory measurements of biomass-burning emissions: 2. First intercomparison of open-path FTIR, and GC-MS/FID/ECD, J. Geophys. Res., 109 (D2), D02311, http://doi.org/10.1029/2003JD003874, 2004.

Cicerone, R. J., and Zellner, R.: The atmospheric chemistry of hydrogen cyanide (HCN), J. Geophys. Res., 88 (C15), 10689-10696, http://doi.org/10.1029/JC088iC15p10689, 1983.

Coggon, M. M., Veres, P. R., Yuan, B., Koss, A., Warneke, C., Gilman, J. B., Lerner, B. M., Peischl, J., Aikin, K. C., Stockwell, C. E., Hatch, L. E., Ryerson, T. B., Roberts, J. M., Yokelson, R. J., and de Gouw, J. A.: Emissions of nitrogen-containing organic compounds from the burning of herbaceous and arboraceous biomass: Fuel composition dependence and the variability of commonly used nitrile tracers, Geophys. Res. Lett., 43(18), 9903–9912, doi:10.1002/2016GL070562, 2016.

Collard, F. X., and Blin, J.: A review on pyrolysis of biomass constituents: Mechanisms and composition of the products obtained from the conversion of cellulose, hemicelluloses and lignin, Renew. Sustainable Energy Rev., 38, 594-608, http://doi.org/10.1016/j.rser.2014.06.013, 2014.

Donahue, N. M., Epstein, S. A., Pandis, S. N., and Robinson, A. L.: A two-dimensional volatility basis set: 1. Organic-aerosol mixing thermodynamics, Atmos. Chem., Phys., 11, 3303-3318, http://doi.org/10.5194/acp-11-3303-2011, 2011.

Gilman, J. B., Lerner, B. M., Kuster, W. C., Goldan, P. D., Warneke, C., Veres, P. R., Roberts, J. M., de Gouw J. A., Burling, I. R., and Yokelson, R. J.: Biomass burning emissions and potential air quality impacts of volatile organic compounds and other trace gases from fuels common in the US, *Atmos. Chem. Phys*., 15 (24), 13915-13938, http://doi.org/10.5194/acp-15-13915-2015, 2015.

Haidar, N. F., Patterson, J. M., Moors, M., and Smith, W. T.: Effects of structure on pyrolysis gases from amino acids, J. Agric. Food. Chem., 29 (1), 163-165, http://doi.org/10.1021/jf00103a040, 1981.

Hansson, K.-M., Samuelsson, J., Tullin, C. and Åmand, L.-E.: Formation of HNCO, HCN, and NH3 from the pyrolysis of bark and nitrogen-containing model compounds, Combust. Flame, 137 (3), 265–277, doi:10.1016/J.COMBUSTFLAME.2004.01.005, 2004.

737 Haslett, S. L., Thomas, J. C., Morgan, W. T., Hadden, R., Liu, D., Allan, J. D., Williams, P. I.,
738 Sekou, K., Liousse, C., and Coe, H.: Highly-controlled, reproducible measurements of aerosol
739 emissions from African biomass combustion, Atmos. Chem. Phys. Discuss.,
740 http://doi.org/10.5194/acp-2017-679, in review, 2017.
741 Hatch, L. E., Luo, W., Pankow, J. F., Yokelson, R. J., Stockwell, C. E., and Barsanti, K. C.:
742 Identification and quantification of gaseous organic compounds emitted from biomass
743 burning using two-dimensional gas chromatography–time-of-flight mass spectrometry, Atmos.
744 Chem. Phys., 15, 1865-1899, https://doi.org/10.5194/acp-15-1865-2015, 2015.
745 Hatch, L. E., Yokelson, R. J., Stockwell, C. E., Veres, P. R., Simpson, I. J., Blake, D. R.,
746 Orlando, J. J., and 724 Barsanti, K. C.: Multi-instrument comparison and compilation of non-
747 methane organic gas emissions from biomass burning and implications for smoke-derived
748 secondary organic aerosol precursors, Atmos. Chem. Phys., 17, 1471-1489, 10.5194/acp-17-
749 1471-2017, 2017.
750 Houser, T. J., McCarville, and M. E., Biftu, T.: Kinetics of the thermal decomposition of
751 pyridine in a flow system, Int. J. Chem. Kinet., 12 (8), 555-568,
752 http://doi.org/10.1002/kin.550120806, 1980.
753 Jaffe, D. A., and Wigder, N. L.: Ozone production from wildfires: A critical review, Atmos.
754 Environ., 51, 1-10, http://doi.org/10.1016/j.atmosenv.2011.11.063, 2012.
755 Johnson, W. R., and Kan, J. C.: Mechanisms of hydrogen cyanide formation from the pyrolysis
756 of amino acids and related compounds, J. Org. Chem., 36 (1), 189-192,
757 http://doi.org/10.1021/jo00800a038, 1971.
758 Kirk, T. K., and Cowling, E. B.: Biological decomposition of solid wood, Adv. Chem., 207 (12),
759 455-487, http://doi.org/10.1021/ba-1984-0207.ch012, 1984.
760 Koss, A. R., Sekimoto, K., Gilman, J. B., Selimovic, V., Coggon, M. M., Zarzana, K. J., Yuan,
761 B., Lerner, B. M., Brown, S. S., Jimenez, J. L., Krechmer, J., Roberts, J. M., Warneke, C.,
762 Yokelson, R. J., and de Gouw, J.: Non-methane organic gas emissions from biomass burning:
763 identification, quantification, and emission factors from PTR-ToF during the FIREX 2016
764 laboratory experiment, Atmos. Chem. Phys., 18, 3299-3319, https://doi.org/10.5194/acp-18-
765 3299-2018, 2018.

766 Leppälahti, J., and Koljonen, T.: Nitrogen evolution from coal, peat and wood during
767 gasification: Literature review, Fuel Process. Technol., 43, 1-45, http://doi.org/10.1016/0378-
768 3820(94)00123-B, 1995.
769 Li, Y., Pöschl, U., and Shiraiwa, M.: Molecular corridors and parameterizations of volatility in
770 the chemical evolution of organic aerosols, Atmos. Chem. Phys., 16 (5), 3327-3344,
771 http://doi.org/10.5194/acp-16-3327-2016, 2016.
772 Lim, C., Hagan, D., Cappa, C., Coggon, M., Koss, A., Sekimoto, K., de Gouw, J., Warneke, C.,
773 Kroll, J. Laboratory studies on the aging of biomass burning emissions: chemical evolution
774 and secondary organic aerosol yield, in preparation, 2018.
775 Liu, W. -J., Li, W. -W., Jiang, H., and Yu, H. -Q.: Fates of chemical elements in biomass during
776 its pyrolysis, Chem. Rev., 117 (9), 6367-6398, http://doi.org/10.1021/acs.chemrev.6b00647,
777 2016.
778 Mackie, J. C., Colket, M. B., III, and Nelson, P. F.: Shock tube pyrolysis of pyridine, J. Phys.
779 Chem., 94 (10), 4099-4106, http://doi.org/10.1021/j100373a040, 1990.
780 Manion, J. A., Huie, R. E., Levin, R. D., Burgess D. R., Jr., Orkin, V. L., Tsang, W., McGivern,
781 W. S., Hudgens, J. W., Knyazev, V. D., Atkinson, D. B., Chai, E., Tereza, A. M., Lin, C. –Y.,
782 Allison, T. C., Mallard, W. G., Westley, F., Herron, J. T., Hampson, R. F., and Frizzell, D. H.:
783 NIST Chemical Kinetics Database, NIST Standard Reference Database 17, Version 7.0 (Web
784 Version), Release 1.6.8, Data version 2015.12, National Institute of Standards and
785 Technology, Gaithersburg, Maryland, 20899-8320. Web address: http://kinetics.nist.gov/,
786 last access: 28 November 2017, 2017.
787 Naeher, L. P., Brauer, M., Lipsett, M., Zelikoff, J. T., Simpson, C. D., Koenig, J. Q., and Smith,
788 K. R.: Woodsmoke health effects: A review, Inhal. Toxicol., 19 (1), 67-106,
789 https://doi.org/10.1080/08958370600985875, 2007.
790 NIST Chemistry WebBook, Web address: http://webbook.nist.gov/chemistry/, last access: 28
791 November 2017, 2017.
792 Paatero, P., and Tapper, U.: Positive matrix factorization: A non-negative factor model with
793 optimal utilization of error estimates of data values, *Environmetrics*, 5 (2), 111-126,
794 http://doi.org/10.1002/env.3170050203, 1994.
795 Paatero, P.: Least squares formulation of robust non-negative factor analysis, Chemometr. Intell.
796 Lab., 37 (1), 23-35, https://doi.org/10.1016/S0169-7439(96)00044-5, 1997.

797 Pagonis, D., Krechmer, J. E., de Gouw, J. A., Jimenez, J. L. and Ziemann, P. J.: Effects of gas-
798 wall partitioning in Teflon tubing and instrumentation on time-resolved measurements of gas-
799 phase organic compounds, Atmos. Meas. Tech., 10, 4687–4696, doi:10.5194/amt-2017-279,
800 2017.
801 Patterson, J. M., Tsamasfyros, A., and Smith, W. T.: Pyrolysis of pyrrole, J. Heterocycle Chem.,
802 5 (5), 727-729, http://doi.org/10.1002/jhet.5570050527, 1968.
803 Reardon, J.: Duff. *In:* FireWords: Fire Science Glossary [electronic]. U.S. Department of
804 Agriculture, Forest Service, Rocky Mountina Research Station, Fire Science Laboratory
805 (Producer). Available: http://www.firewords.net, last update 2007.
806 Reece, S. M., Sinha, A., and Grieshop, A. P.: Primary and photochemically aged aerosol
807 emissions from biomass cookstoves: Chemical and physical characterization, Environ. Sci.
808 Technol., 51 (16), 9379-9390, http://doi.org/10.1021/acs.est.7b01881, 2017.
809 Ren, Q., Zhao, C., Chen, X., Duan, L., Li, Y. and Ma, C.: $NO_x$ and $N_2O$ precursors ($NH_3$ and
810 HCN) from biomass pyrolysis: Co-pyrolysis of amino acids and cellulose, hemicellulose and
811 lignin, Proc. Combust. Inst., 33(2), 1715–1722, http://doi.org/10.1016/J.PROCI.2010.06.033,
812 2011.
813 Ren, Q., and Zhao, C.: Evolution of fuel-N in gas phase during biomass pyrolysis, Renew. Sust.
814 Energ. Rev., 50, 408-418, http://doi.org/10.1016/j.rser.2015.05.043, 2015.
815 Roberts, J. M, Veres, P. R., Cochran, A. K., Warneke, C., Burling, I. R., Yokelson, R. J., Lerner,
816 B., Gilman, J. B., Kuster, W. C., Fall, R., and de Gouw, J.: Isocyanic acid in the atmosphere
817 and its possible link to smoke-related health effects, Proc. Natl. Acad. Sci., 208 (22), 8966-
818 8971, http://doi.org/10.1073/pnas.1103352108, 2011.
819 Rumble, J. R. CRC Handbook of Chemistry and Physics, 98$^{th}$ Ed. (2017-2018).
820 Schulten, H. –R. and Schnitzer, M.: The chemistry of soil organic nitrogen: a review, Biol. Fert.
821 Soils., 26, 1-15, 1997.
822 Selimovic, V., Yokelson, R. J., Warneke, C., Roberts, J. M., de Gouw, J., Reardon, J., and
823 Griffith, D. W. T.: Aerosol optical properties and trace gas emissions by PAX and OP-FTIR
824 for laboratory-simulated western US wildfires during FIREX, *Atmos. Chem. Phys.*, 18, 2929-
825 2948, http://doi.org/10.5194/acp-18-2929-2018, 2018.
826 Stockwell, C. E., Veres, P. R., Williams, J., and Yokelson, R. J.: Characterization of biomass
827 burning emissions from cooking fires, peat, crop residue, and other fuels with high-resolution

proton-transfer-reaction time-of-flight mass spectrometry, Atmos. Chem. Phys., 15 (15), 845-865, http://doi.org/10.5194/acp-15-845-2015, 2015.

Ulbrich, I. M., Canagaratna, M. R., Zhang, Q., Worsnop, D. R., and Jimenez, J. L.: Interpretation of organic components from Positive Matrix Factorization of aerosol mass spectrometric data, Amos. Chem. Phys., 9 (9), 2891-2918, http://doi.org/10.5194/acp-9-2891-2009, 2009.

Yaws, C. L.: The Yaws Handbook of Vapor Pressure: Antoine Coefficients, Elsevier Science, 2015.

Yee, L. D., Kautzman, K. E., Loza, C. L., Schilling, K. A., Coggon, M. M., Chhabra, P. S., Chan, M. N., Chan, A. W. H., Hersey, S. P., Crounse, J. D., Wennberg, P. O., Flagan, R. C., and Seinfeld, J. H.: Secondary organic aerosol formation from biomass burning intermediates: phenol and methoxyphenols, Atmos. Chem. Phys., 13 (16), 8019–8043, http://doi.org/10.5194/acp-13-8019-2013, 2013.

Yokelson, R. J., Griffith, D. W. T., and Ward, D. E.: Open-path Fourier transform infrared studies of large-scale laboratory biomass fires, J. Geophys. Res. Atmos., 101 (D15), 21067-21080, http://doi.org/10.1029/96JD01800, 1996.

Yokelson, R. J., Susott, R., Ward, D. E., Reardon, J., and Griffith, D. W. T.: Emissions from smoldering combustion of biomass measured by open-path Fourier transform infrared spectroscopy, J. Geophys. Res. Atmos., 102 (D15), 18865-18877, http://doi.org/10.1029/97JD00852, 1997.

Yokelson, R. J., Crounse, J. D., de Carlo, P. F., Karl, T., Urbanski, S., Atlas, E., Campos, T., Shinozuka, Y., Kapustin, V., Clarke, A. D., Weinheimer, A., Knapp, D. J., Montzka, D. D., Holloway, J., Weibring, P., Flocke, F., Zheng, W., Toohey, D., Wennberg, P. O., Wiedinmyer, C., Mauldin, L., Fried, A., Richter, D., Walega, J., Jimenez, J. L., Adachi, K., Buseck, P. R., Hall, S. R., and Shetter, R.: Emissions from biomass burning in the Yucatan, Atmos. Chem. Phys., 9 (15), 5785-5812, http://doi.org/10.5194/acp-9-5785-2009, 2009.

Yuan, B., Koss, A., Warneke, C., Gilman, J. B., Lerner, B. M., Stark, H., and de Gouw, J. A.: A high resolution time-of-flight chemical ionization mass spectrometer utilizing hydronium ions ($H_3O^+$ ToF-CIMS) for measurements of volatile organic compounds in the atmosphere, Atmos. Meas. Tech., 9 (6), 2735-2752, http://doi.org/10.5194/amt-9-2735-2016, 2016.

857 Yuan, B., Koss, A., Warneke, C., Coggon, M., Sekimoto, K., and de Gouw, J. A.: Proton-
858 transfer-reaction mass spectrometry: Applications in atmospheric sciences, Chem. Rev., 117
859 (21), 13187-13229, http://doi.org/10.1021/acs.chemrev.7b00325, 2017.

**Table 1. (a) Data numbers and corresponding details of 15 different fuels used in PMF analysis. (b) Average MCE and fuel moisture content. (c) Residuals of 2-factor PMF solutions. (d) Correlation with average VOC emission profile (Figure 3).**

| Fuel | (a) Data number for consolidated PMF | | | | (b) Fire characteristics | | (c) Residual [%] [a] | (d) Correlation with average VOC emission profile (Figure 3) | | | |
|---|---|---|---|---|---|---|---|---|---|---|---|
| | | | | | | | | High-temperature pyrolysis factor | | Low-temperature pyrolysis factor | |
| | Total | Detail | | | MCE | Moiture content | Average ± STDV (maximum, minimum) | Slope | Correlation coefficient ($r^2$) | Slope | Correlation coefficient ($r^2$) |
| 1. Ponderosa pine | 10 | Realistic | 5 | (Fire 01, 02, 37, 59, 72) | 0.913-0.940 | 24.3-31.8% | 15.7 ± 7.6 (28.9, 7.7) | 0.976 ± 0.004 | 0.9393 | 1.012 ± 0.005 | 0.9245 |
| | | Canopy | 2 | (Fire 19, 39) | 0.904-0.935 | 40.4-51.1% | | | | | |
| | | Litter | 1 | (Fire 38) | 0.945 | 6.2% | | | | | |
| | | Rotten log | 2 | (Fire 13, 73) | 0.932-0.957 | 2.9-5.7% | | | | | |
| 2. Lodgepole pine | 7 | Realistic | 4 | (Fire 06, 07, 58, 63) | 0.927-0.943 | 20.3-24.4% | 14.8 ± 4.9 (23.3, 10.9) | 0.990 ± 0.004 | 0.9586 | 0.990 ± 0.002 | 0.9716 |
| | | Canopy | 1 | (Fire 40) | 0.924 | 49.30% | | | | | |
| | | Litter | 2 | (Fire 21, 41) | 0.925-0.938 | 7.0-10.5% | | | | | |
| 3. Loblolly pine | 2 | Litter | 2 | (Fire 35, 53) | 0.922-0.929 | 5.4-10.9% | 6.3 ± 0.3 (6.6, 6.1) | 0.989 ± 0.007 | 0.8662 | 0.960 ± 0.004 | 0.8862 |
| 4. Douglas fir | 4 | Realistic | 2 | (Fire 14, 57) | 0.926-0.951 | 23.3-25.7% | 21.2 ± 9.3 (34.9, 14.9) | 0.996 ± 0.004 | 0.9508 | 0.999 ± 0.003 | 0.9563 |
| | | Canopy | 1 | (Fire 18) | 0.928 | 50.3% | | | | | |
| | | Litter | 1 | (Fire 43) | 0.951 | 3.0% | | | | | |
| 5. Engelmann spruce | 3 | Realistic | 1 | (Fire 08) | 0.920 | 13.0% | 20.5 ± 2.4 (22.2, 18.8) [b] | 0.999 ± 0.006 [b] | 0.9019 [b] | 0.960 ± 0.004 [b] | 0.9004 [b] |
| | | Canopy | 1 | (Fire 25) | 0.950 | 34.0% | | | | | |
| | | Duff | 1 | (Fire 26) | 0.817 | 0.6% | 82.0 | - | - | - | - |
| 6. Subalpine fir | 6 | Realistic | 2 | (Fire 47, 67) | 0.932-0.942 | 32.8-35.6% | 23.0 ± 14.1 (45.2, 9.1) [b] | 1.001 ± 0.005 [b] | 0.9359 [b] | 0.999 ± 0.003 [b] | 0.9547 [b] |
| | | Canopy | 2 | (Fire 15, 23) | 0.886-0.947 | 17.6-55.5% | | | | | |
| | | Litter | 1 | (Fire 51) | 0.906 | 6.6% | | | | | |
| | | Duff | 1 | (Fire 56) | 0.886 | 0.9% | 87.0 | - | - | - | - |
| 7. Juniper | 2 | Canopy | 2 | (Fire 68, 75) | 0.928-0.939 | 45.0-48.0% | 6.4 ± 3.0 (8.5, 4.3) | 1.016 ± 0.006 | 0.8872 | 0.971 ± 0.004 | 0.9010 |
| 8. Bear grass | 1 | - | | (Fire 62) | 0.897 | 55.1% | 5.6 | 1.039 ± 0.006 | 0.8847 | 1.006 ± 0.004 | 0.9174 |
| 9. Excelsior | 2 | - | | (Fire 49, 61) | 0.945-0.971 | 3.9-5.4% | 6.2 ± 3.0 (8.3, 4.0) | 1.04 ± 0.01 | 0.6806 | 1.012 ± 0.007 | 0.8521 |
| 10. Ceatnothus | 2 | Shrub | 2 | (Fire 69, 74) | 0.942-0.947 | 17.7-27.9% | 10.2 ± 1.1 (11.0, 9.5) | 1.000 ± 0.007 | 0.8416 | 1.030 ± 0.006 | 0.8985 |
| 11. Chamise (contaminated) | 3 | Canopy | 3 | (Fire 24, 29, 46) | 0.948-0.959 | 10.9-16.1% | 13.1 ± 3.9 (16.0, 8.6) | 1.037 ± 0.006 | 0.8951 | 1.044 ± 0.004 | 0.9477 |
| 12. Chamise (uncontaminated) | 3 | Canopy | 3 | (Fire 27, 32, 48) | 0.946-0.954 | 6.2-17.1% | 12.6 ± 2.0 (14.2, 10.4) | 1.017 ± 0.005 | 0.9322 | 1.024 ± 0.004 | 0.9299 |
| 13. Manzanita (contaminated) | 2 | Canopy | 2 | (Fire 30, 33) | 0.962-0.963 | 23.5-26.7% | 13.0 ± 1.1 (13.8, 12.3) | 0.997 ± 0.004 | 0.9347 | 1.034 ± 0.004 | 0.9504 |
| 14. Manzanita (uncontaminated) | 2 | Canopy | 2 | (Fire 28, 34) | 0.963-0.964 | 25.7-26.3% | 7.3 ± 1.1 (8.0, 6.5) | 1.015 ± 0.005 | 0.9229 | 1.043 ± 0.005 | 0.9224 |
| 15. Sagebrush | 2 | Shrub | 2 | (Fire 66, 71) | 0.919-0.922 | 37.8-54.2% | 7.0 ± 2.1 (8.5, 5.6) | 0.993 ± 0.005 | 0.9046 | 1.011 ± 0.004 | 0.9306 |

[a] Residual [%] = [Total measured ion signal - Total synthetic ion signal of high- and low-temperature factors] / Total measured ion signal x 100

[b] "Duff" data is excluded.

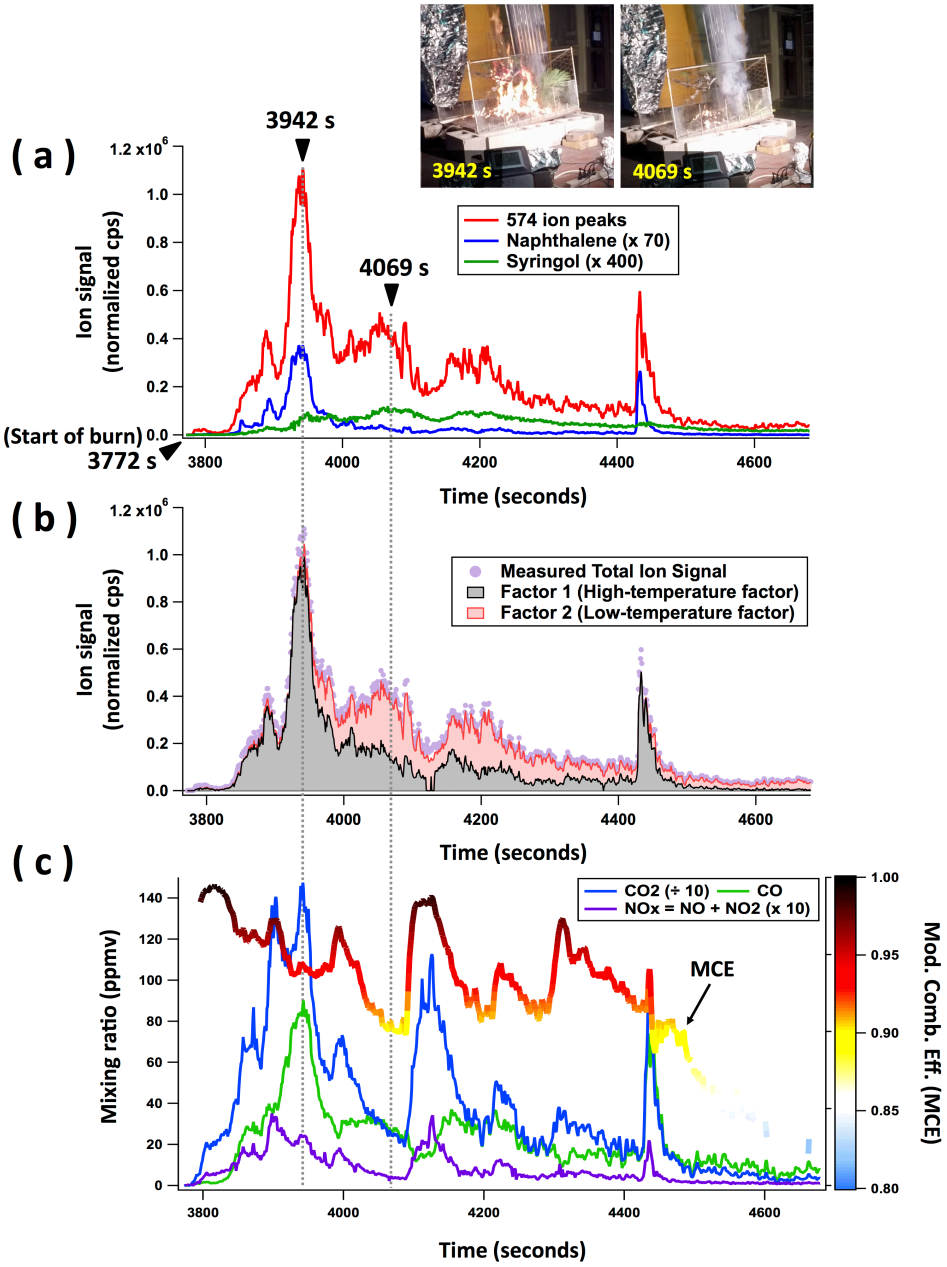


**Figure 1. Results for an example burn of Ponderosa pine realistic mixture (Fire #37). (a) Time series of ion signals of 574 ion peaks, naphthalene ($C_{10}H_8 \cdot H^+$, *m/z* 129.070), and syringol ($C_8H_{10}O_3 \cdot H^+$, *m/z* 155.070). (b) PMF results of 2-factor solution. The grey and pink colors are stacked, not overlapped. (c) Time series of mixing ratios of $CO_2$, CO, and $NO_x$ measured by open-path Fourier transform infrared (OP-FTIR) optical spectroscopy and the modified combustion efficiency (MCE) (Selimovic et al., 2018). The MCE trace is colored by the key and scale on the right.**

## ( a ) Ponderosa (Fire 72) vs. Ponderosa (Fire 02)

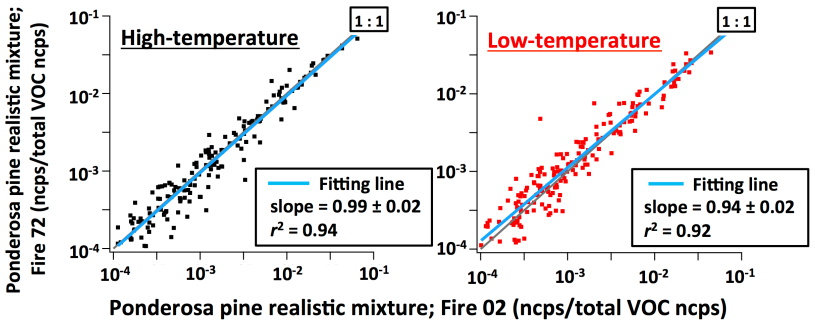


## ( b ) Douglas fir vs. Ponderosa pine

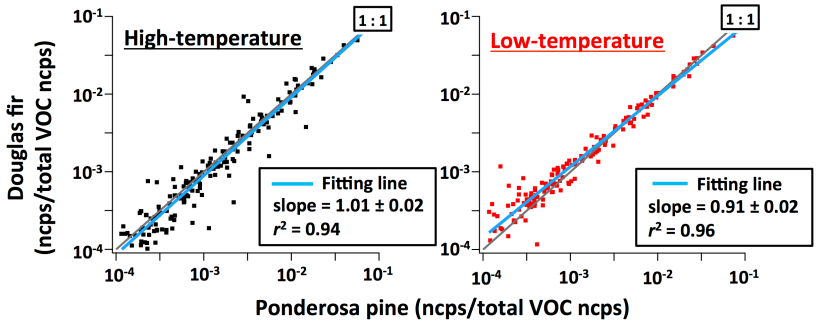


## ( c ) Manzanita vs. Ponderosa pine

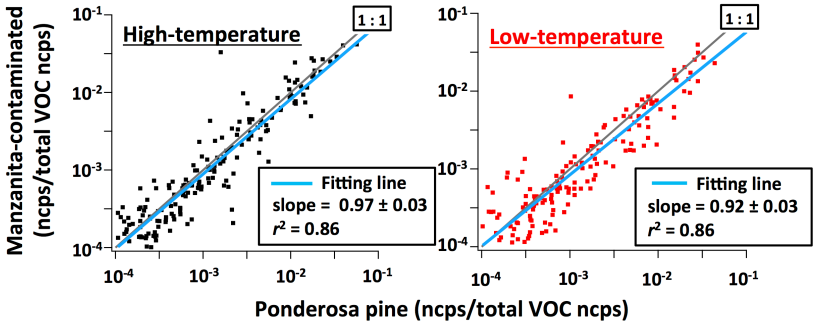


## ( d ) Bear grass vs. Ponderosa pine

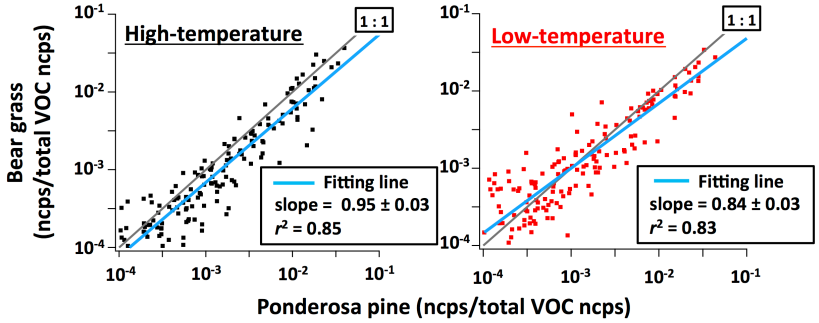


---

## ( e ) Low-temperature vs. High-temperature pyrolysis factor

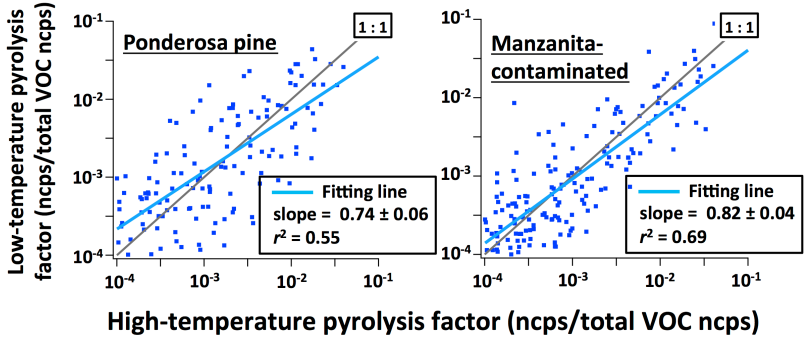

**Figure 2. Comparison of mass spectral profiles: (a) Ponderosa pine realistic mixture (Fire #72) vs. Ponderosa pine realistic mixture (Fire #02) for high- and low-temperature pyrolysis factors. (In this case, PMF was separately performed for data of Fire #02 and #72.) (b) Douglas fir vs. Ponderosa pine for high- and low-temperature factors. (c) Manzanita (contaminated) vs. Ponderosa pine for both the factors. (d) Bear grass vs. Ponderosa pine for both the factors. (e) Low- vs. high-temperature pyrolysis factor for Ponderosa pine and Manzanita (contaminated). Data points in individual panels correspond to well-fitted 434 ion peaks. Slope and correlation coefficient ($r^2$) are obtained using logarithmic fraction, i.e., log(ncps/total VOC ncps).**

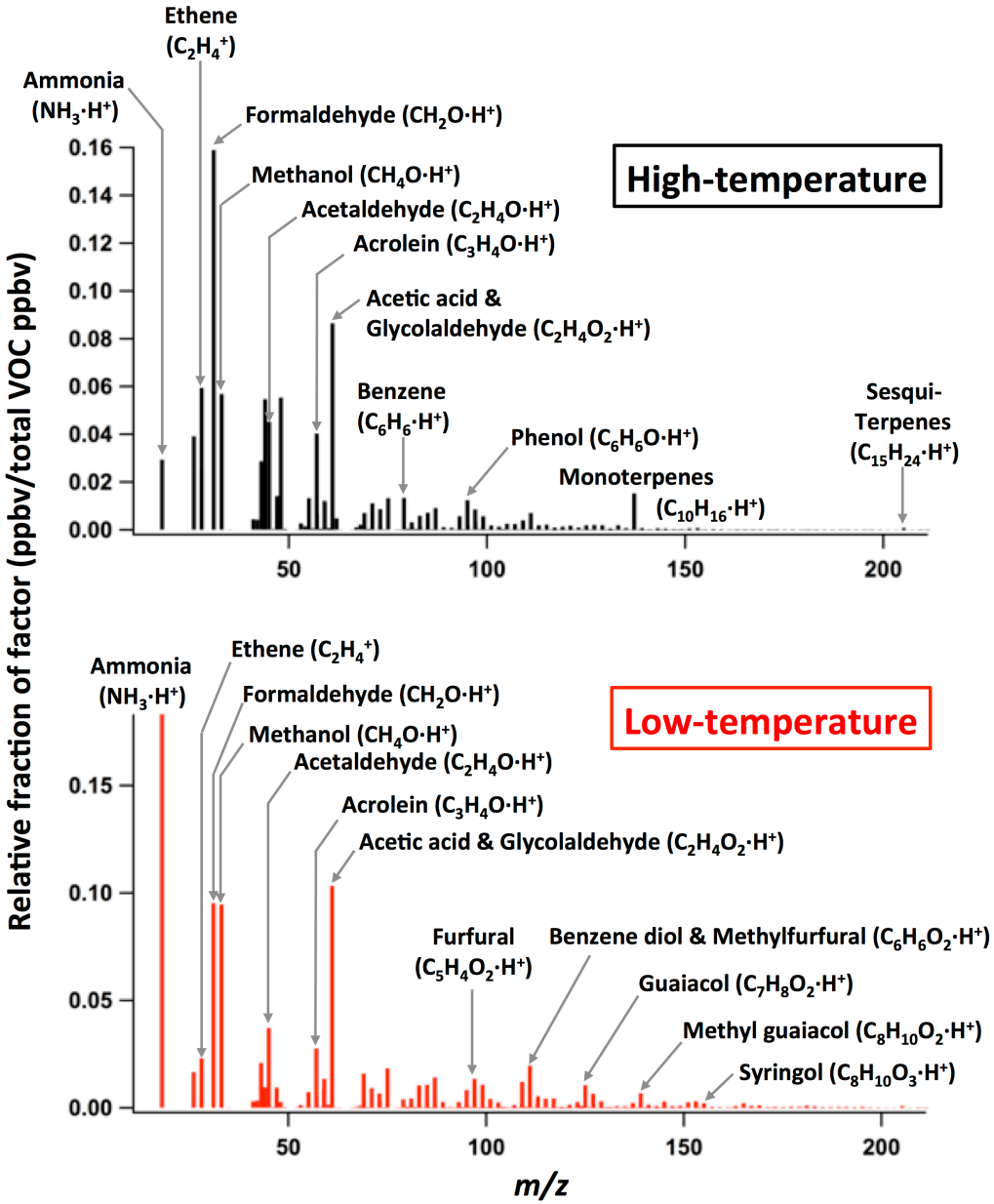


**Figure 3. Average VOC emission profiles of high- and low-temperature pyrolysis factors, obtained using consolidated PMF results of 15 different fuels.**

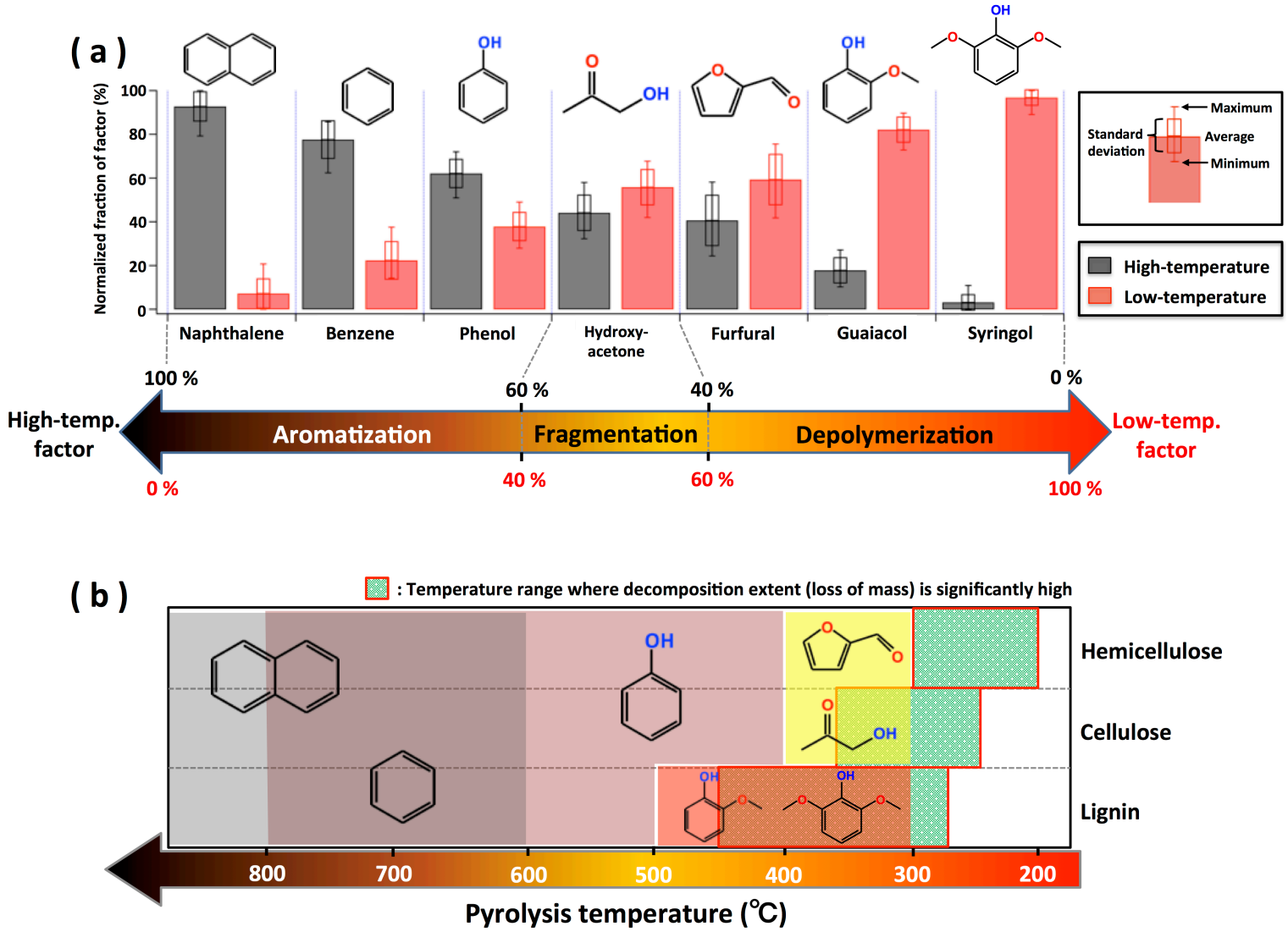


**Figure 4. (a) Normalized fraction of factors for selected biomass pyrolysis products, obtained using PMF results of 15 different fuels. (b) Diagram of the relationship between pyrolysis temperature and products for hemicellulose, cellulose, and lignin, as reported in the literature (Collard and Blin, 2014). Individual color bars show the temperature range to form specific products described by chemical structures.**

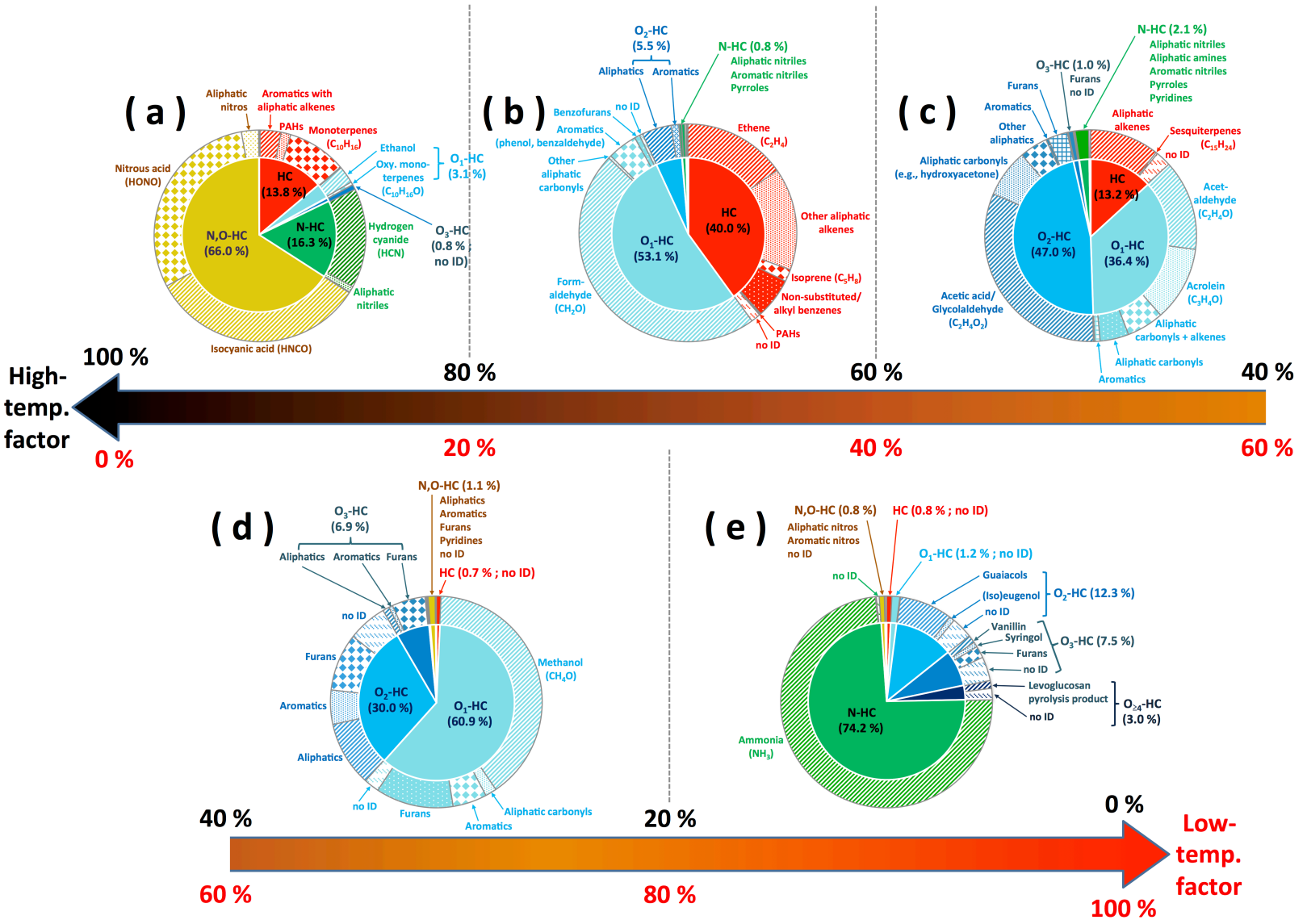
( a )
Aliphatic nitros
Aromatics with aliphatic alkenes
PAHs
Monoterpenes ($C_{10}H_{16}$)
Ethanol
Oxy. mono-terpenes ($C_{10}H_{16}O$)
$O_1$-HC (3.1 %)
Nitrous acid (HONO)
HC (13.8 %)
N-HC (16.3 %)
N,O-HC (66.0 %)
Hydrogen cyanide (HCN)
$O_3$-HC (0.8 % ; no ID)
Aliphatic nitriles
Isocyanic acid (HNCO)
( b )
$O_2$-HC (5.5 %)
Aliphatics
Aromatics
N-HC (0.8 %)
Aliphatic nitriles
Aromatic nitriles
Pyrroles
Benzofurans
no ID
Aromatics (phenol, benzaldehyde)
Ethene ($C_2H_4$)
Other aliphatic carbonyls
HC (40.0 %)
Other aliphatic alkenes
$O_1$-HC (53.1 %)
Form-aldehyde ($CH_2O$)
Isoprene ($C_5H_8$)
Non-substituted/ alkyl benzenes
PAHs
no ID
( c )
N-HC (2.1 %)
Aliphatic nitriles
Aliphatic amines
Aromatic nitriles
Pyrroles
Pyridines
$O_3$-HC (1.0 %)
Furans
Furans
no ID
Aromatics
Other aliphatics
Aliphatic alkenes
Sesquiterpenes ($C_{15}H_{24}$)
no ID
Aliphatic carbonyls (e.g., hydroxyacetone)
HC (13.2 %)
Acet-aldehyde ($C_2H_4O$)
$O_2$-HC (47.0 %)
$O_1$-HC (36.4 %)
Acrolein ($C_3H_4O$)
Acetic acid/ Glycolaldehyde ($C_2H_4O_2$)
Aliphatic carbonyls + alkenes
Aliphatic carbonyls
Aromatics
High-temp. factor
100 %
80 %
60 %
40 %
0 %
20 %
40 %
60 %
( d )
N,O-HC (1.1 %)
Aliphatics
Aromatics
Furans
Pyridines
no ID
$O_3$-HC (6.9 %)
Aliphatics
Aromatics
Furans
HC (0.7 % ; no ID)
no ID
Furans
Aromatics
$O_2$-HC (30.0 %)
$O_1$-HC (60.9 %)
Methanol ($CH_4O$)
Aliphatics
no ID
Furans
Aromatics
Aliphatic carbonyls
( e )
N,O-HC (0.8 %)
Aliphatic nitros
Aromatic nitros
no ID
HC (0.8 % ; no ID)
$O_1$-HC (1.2 % ; no ID)
no ID
Guaiacols
(Iso)eugenol
$O_2$-HC (12.3 %)
no ID
Vanillin
Syringol
Furans
no ID
$O_3$-HC (7.5 %)
Levoglucosan
pyrolysis product
no ID
$O_{\geq 4}$-HC (3.0 %)
N-HC (74.2 %)
Ammonia ($NH_3$)
40 %
20 %
0 %
60 %
80 %
100 %
Low-temp. factor
Hydrocarbons (HC)
N-containing hydrocarbons (N-HC)
N and O-containing hydrocarbons (N,O-HC)
O-containing hydrocarbons ($O_n$-HC, $n$ : number of oxygen atom)
$n$ = 1
$n$ = 2
$n$ = 3
$n \geq 4$

**Figure 5. Contributions, shown as normalized fractions, of VOCs relative to the high- and low-temperature factors: (a) $F_{\text{High-T}}$ = 100-80% and $F_{\text{Low-T}}$ = 0-20%, (b) $F_{\text{High-T}}$ = 80-60% and $F_{\text{Low-T}}$ = 20-40%, (c) $F_{\text{High-T}}$ = 60-40% and $F_{\text{Low-T}}$ = 40-60%, (d) $F_{\text{High-T}}$ = 40-20% and $F_{\text{Low-T}}$ = 60-80%, and (e) $F_{\text{High-T}}$ = 20-0% and $F_{\text{Low-T}}$ = 80-100%. In this figure, molar emissions (in units of ppbv) of all the ion peaks in VOC emission profiles (Figure 2b) are described. The inner circle in each pie chart shows the elemental composition of the emissions. The outer circle provides more detailed information on specific compounds, structures, and functionalities found in each group. Details of molar fractions in each category are summarized in Table S2.**

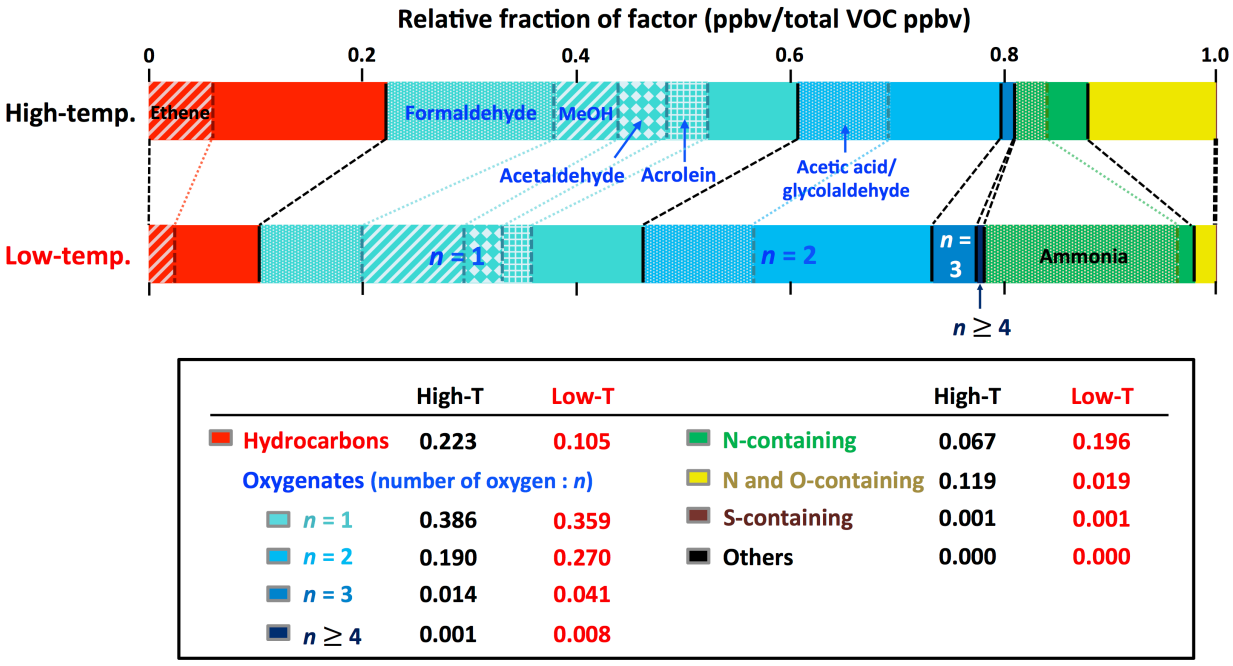


| | High-T | Low-T | | High-T | Low-T |
|---|---|---|---|---|---|
| Hydrocarbons | 0.223 | 0.105 | N-containing | 0.067 | 0.196 |
| Oxygenates (number of oxygen : *n*) | | | N and O-containing | 0.119 | 0.019 |
| *n* = 1 | 0.386 | 0.359 | S-containing | 0.001 | 0.001 |
| *n* = 2 | 0.190 | 0.270 | Others | 0.000 | 0.000 |
| *n* = 3 | 0.014 | 0.041 | | | |
| *n* ≥ 4 | 0.001 | 0.008 | | | |

**Figure 6. VOC composition in the high- and low-temperature emission profiles.**

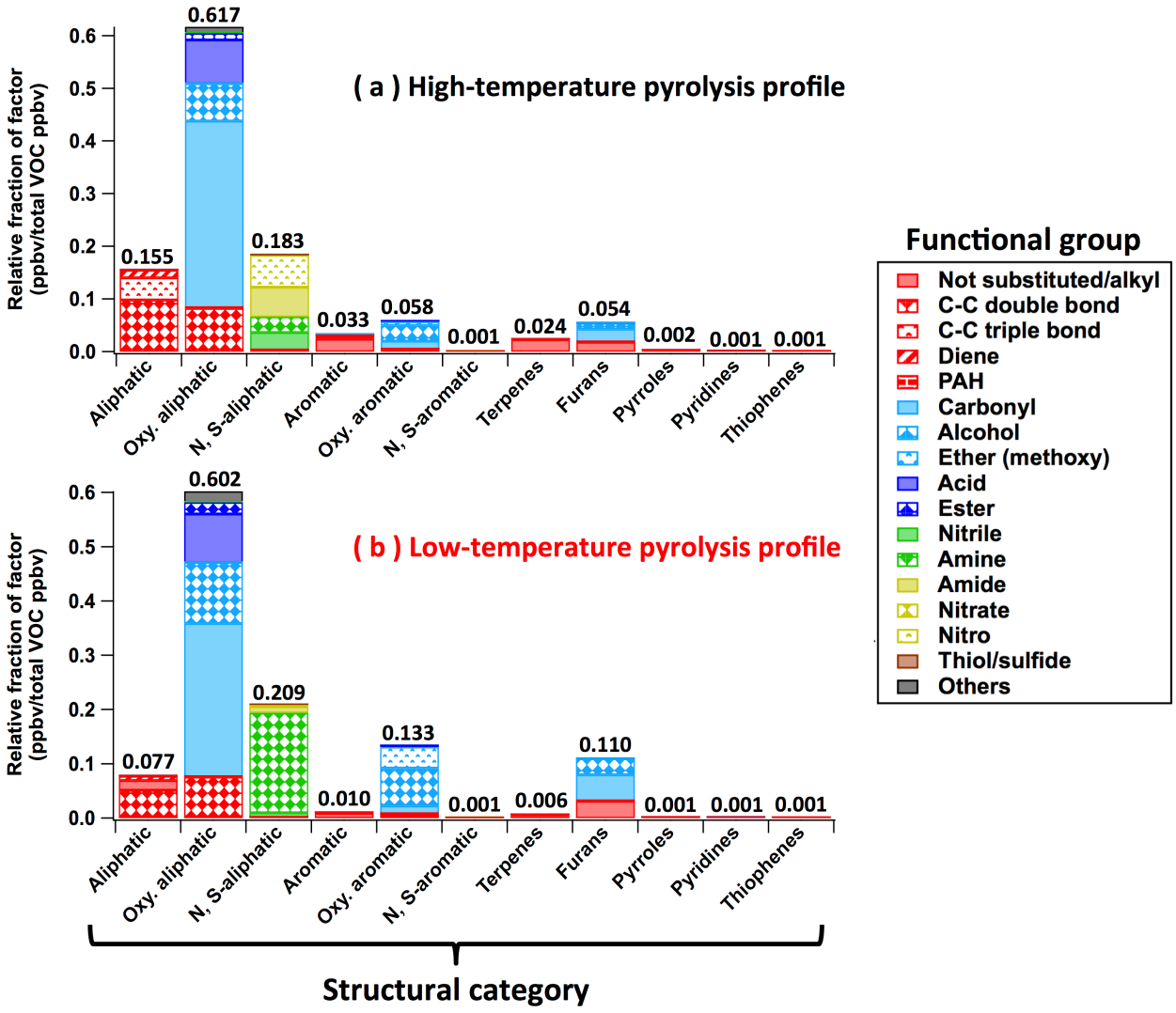


**Figure 7. VOC composition in (a) high-temperature pyrolysis and (b) low-temperature pyrolysis emission profiles (Figure 3) sorted by 11 structural categories and 17 functional groups. Some VOCs have multiple structures. These are counted once in each relevant category. For example, benzofuran is counted in the structural categories of "Oxy. aromatic" and "Furans" as "Not substituted/alkyl" functional group. Structures detected with low abundance (<0.002 ppbv/total VOC ppbv) are mostly not-substituted or alkyl-substituted.**

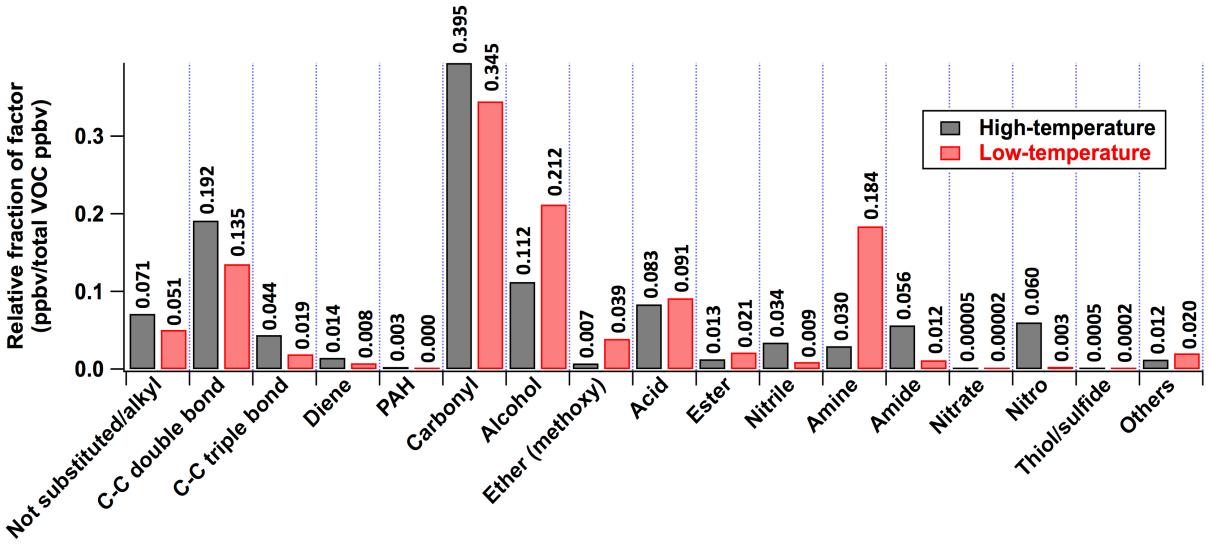


**Figure 8. VOC composition in high- and low-temperature pyrolysis emission profiles (Figure 3) sorted by 17 functional groups. Each group includes various structures and elemental composition. Some VOCs have multiple functional groups. These are counted once in each relevant category. For example, guaiacol is counted in the categories of "Alcohol" and "Ether (methoxy)".**

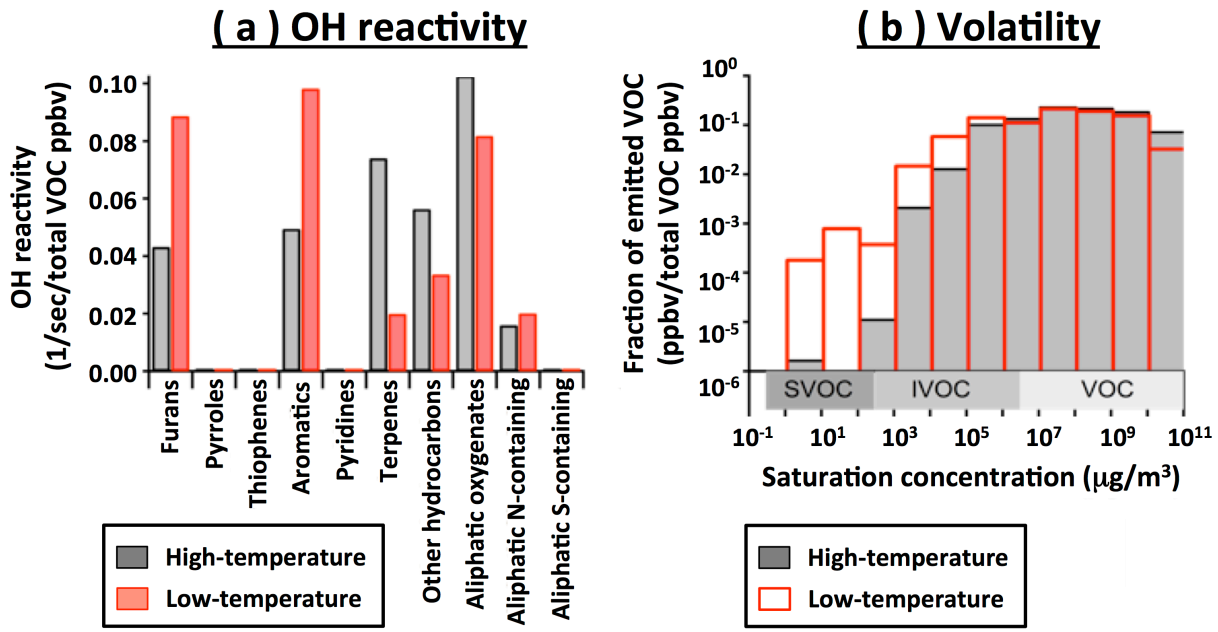


**Figure 9. High- and low-temperature emission profiles compared by (a) OH reactivity and (b) volatility, described by saturation concentration (μg $m^{-3}$).**

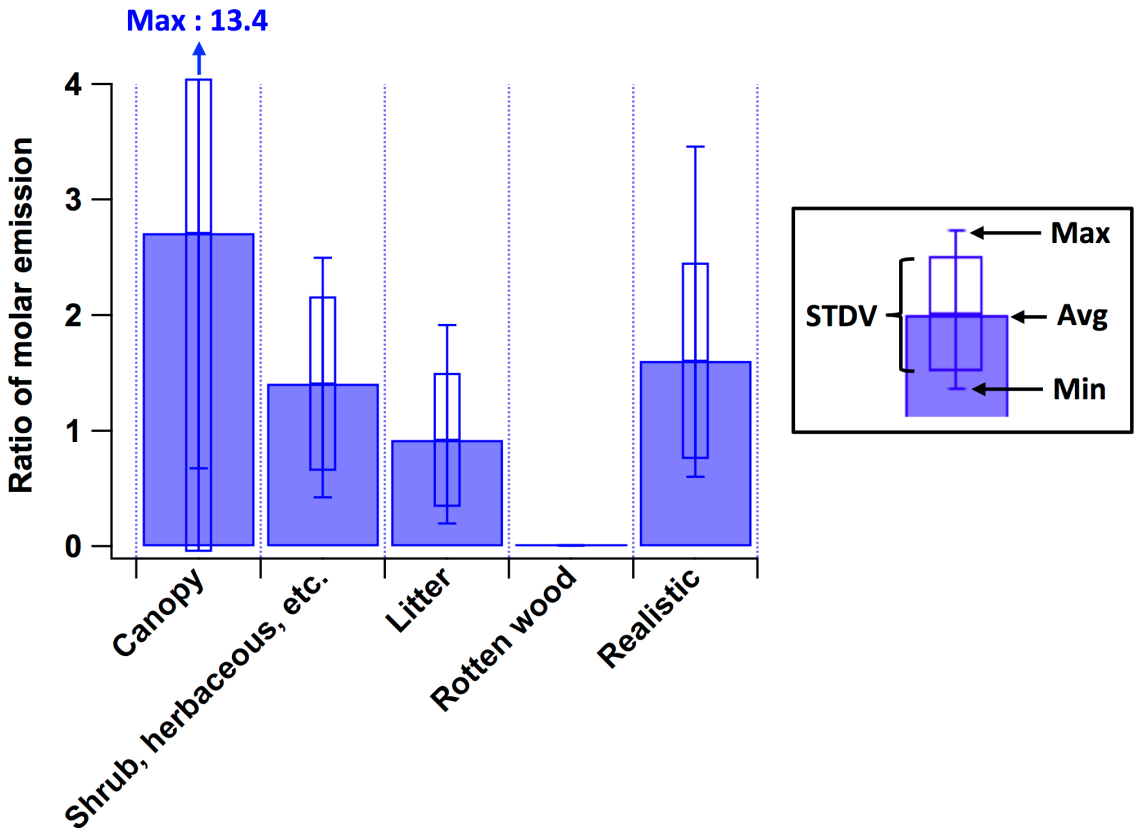


**Figure 10. Ratios of fire-integrated molar emissions of total VOCs from high- to low-temperature pyrolysis ("$\sum VOC_{High\text{-}T}/\sum VOC_{Low\text{-}T}$") for different type fuel parts, obtained using PMF results of 15 different fuels.**

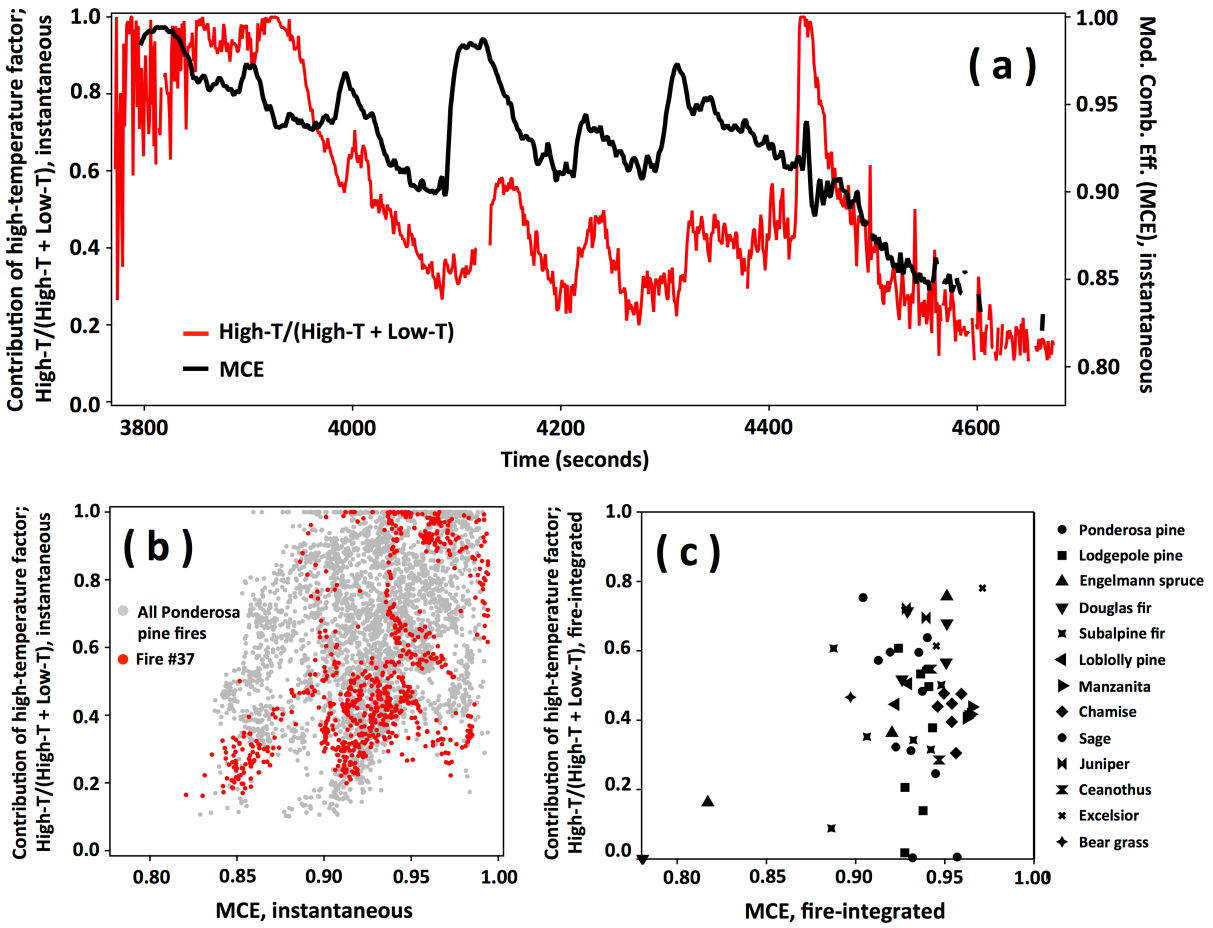


**Figure 11. The comparison of contribution of high-temperature factor versus modified combustion efficiency (MCE). (a) Time series of Fire #37 (Ponderosa pine realistic mixture). (b) Scatter plot of instantaneous high-temperature contribution versus MCE for all Ponderosa pine fires. (c) Scatter plot of fire-integrated high-temperature contribution versus MCE for all fires. Contribution of high-temperature factor was calculated by $\Sigma VOC_{high\text{-}T}/(\Sigma VOC_{high\text{-}T} + \Sigma VOC_{low\text{-}T})$ instantaneously or on a fire-integrated basis.**

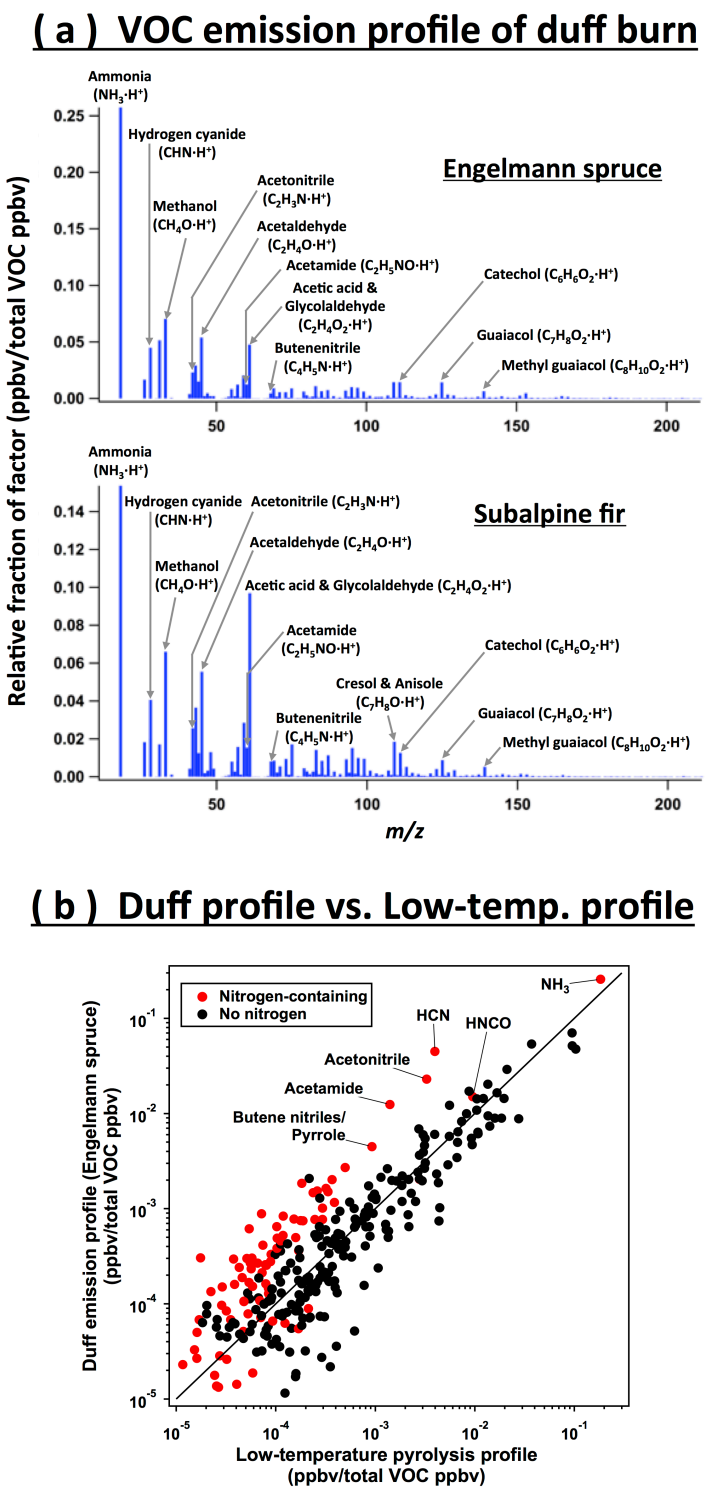


**Figure 12. (a) VOC emission profile of duff burn of Engelmann spruce and Subalpine fir. (b) Scatter plot of duff emission profile (Engelmann spruce) versus average low-temperature pyrolysis profile.**